0022-1554/96/$3.30
The Journal of Histochemistry and Cytochemistry

Vol. 44, No. 5, pp. 445–461, 1996
Printed in U.S.A.

Original Article

Organ Distribution of Aminopeptidase A and Dipeptidyl Peptidase IV in Normal Mice[1]

STEF MENTZEL,[2] HENRI B. P. M. DIJKMAN, JACCO P. H. F. VAN SON, ROBERT A. P. KOENE, and KAREL J. M. ASSMANN

Department of Pathology (SM, HBPMD, JPHFvS, KJMA) and Department of Medicine, Division of Nephrology (RAPK), University Hospital Nijmegen, Nijmegen, The Netherlands.

Received for publication August 31, 1995 and in revised form December 1, 1995; accepted December 10, 1995 (5A3762).

The hydrolases aminopeptidase A and dipeptidyl peptidase IV, both present in the kidney on the brush borders of the proximal tubule epithelial cells and podocytes, are involved in the induction of experimental membranous glomerulonephritis in the mouse. However, little is known about their (co)distribution in other tissues and their function in health and disease. A detailed insight into the localization of these two enzymes is a prerequisite to elucidation of their function. Therefore, we investigated the presence and co-distribution of aminopeptidase A and dipeptidyl peptidase IV by immunohistology with two different rat monoclonal antibodies, the specificity of which was determined by an immunodepletion technique. In addition, the molecular weight of the hydrolases was analyzed by SDS-PAGE after isolation by solid-phase immunoprecipitation from glomeruli, renal brush borders, and thymus. Both hydrolases showed different molecular weights in renal corpuscle, renal brush borders, and thymic cells. A widespread organ distribution of the two hydrolases was observed, with co-localization in kidney, liver, small intestine, thymus, brain, spleen, and lymph nodes, either on the same cells or on different cells in the same organ. This distribution and partial co-localization suggests that the two hydrolases, acting either alone or in concert, have a role in many diverse biological processes. (*J Histochem Cytochem 44:445–461, 1996*)

KEY WORDS: Aminopeptidase A; Dipeptidyl peptidase IV; Organ distribution; Mouse.

Introduction

Antibodies that interact with intrinsic antigens on podocytes can induce a membranous glomerulonephritis, which can be used as an experimental model for the human form of this disease (1,2). One of these antigens which has extensively been studied in the rat is the Heymann antigen (3–5). However, this antigen is not present on mouse podocytes and is therefore not involved in the development of membranous glomerulonephritis in this species (6). We have found that two other antigens present on podocytes, i.e., the hydrolases aminopeptidase A (APA; EC 3.4.11.7) and dipeptidyl peptidase IV (DPP IV; EC 3.4.14.5), can participate as targets in the induction of a passive membranous glomerulonephritis in the mouse (6–9). Both enzymes have also been reported to be involved in other experimental and human forms of nephropathy, such as the renal ablation model (10), passive anti-DPP IV nephritis (11–13), Heymann nephritis (14–16) in the rat, lupus nephritis in the mouse (17,18), and glomerulosclerosis (19), diabetic nephropathy (20), and chronic interstitial nephritis (21,22) in humans.

Both APA and DPP IV are cell membrane-bound hydrolases, assumed to be involved in diverse biological processes such as peptide degradation (23,24) and B- and T-cell differentiation (23,25). Previous studies have shown that APA and DPP IV are also present on various cell types of many organs other than the kidney. Therefore, studies on the organ distribution of APA have been carried out in the rat and mouse with enzyme histochemical methods (26,27) and on a restricted number of organs in the mouse with a monoclonal antibody (MAb) against the BP1/6C3 antigen which was recently identified as APA (28). The organ distribution of DPP IV has been examined in a more or less restricted way in the mouse, rat, and rabbit by enzyme histochemistry (29) or immunohistology using MAbs (13,30,31). Previously, we studied the localization of DPP IV in the mouse with polyclonal antibodies (6,8,31) that may lack the ultimate specificity of MAbs. In our laboratory we have generated a panel of rat MAbs to different antigens present on podocytes, several of which were directed to APA and DPP IV. For this study we selected two clones, ASD-4 and ASD-36, which bind respectively to APA and DPP IV (7). These two MAbs enabled us to study more thoroughly the organ distribution and putative co-localization of APA and DPP IV in the mouse. Because the functional roles of the two enzymes are largely unknown, we studied the organ distribution of APA and DPP IV, thus looking in greater detail at their distribution in kidney and thymus.

[1] Supported by a grant from the Dutch Kidney Foundation (C91.1169).
[2] Correspondence to: S. Mentzel, Dept. of Pathology, University Hospital Nijmegen, PO Box 9101, 6500 HB Nijmegen, The Netherlands.

Materials and Methods

Animals. Balb/c and Balb/c, nu/nu mice were originally obtained from the Jackson Laboratory (Bar Harbor, ME) and were kept in the breeding farm facility of the Central Laboratory of Animals of our university by continuous brother–sister matings. Male Lou rats used for the production of MAbs were obtained from Harlan Olac (Blackthorn, Bicester, UK).

Preparation of Solubilized Suspensions from Renal Brush Borders, Renal Corpuscles, and Thymus. An enriched suspension of mouse renal brush border membrane vesicles from proximal tubule epithelial cells was prepared from Balb/c kidneys according to the method of Malathi et al. (32), using a 2-mM Tris-HCl buffer, pH 7.2, containing 50 mM mannitol, the protease inhibitors EDTA (20 mM), PMSF (1 mM), benzamidine (1 mM), Trasylol (10 U/ml), and 0.02% NaN_3 as described (7). The brush border suspension was solubilized with 2% Triton X-114 in 50 mM Tris-HCl at 4°C for 30 min and subjected to Triton X-114 phase separation at 37°C for 20 min, followed by centrifugation at 300 × g for 5 min (33). The obtained brush border preparation enriched in integral membrane proteins served as immunogen for the production of MAbs. In the immunoprecipitation procedure, a brush border fraction was used that was solubilized with 1% sodium deoxycholate (brush border Doc) in 50 mM Tris-HCl, pH 8.5, with protease inhibitors and was subsequently centrifuged at 100,000 × g for 1 hr at 4°C. For the fluorimetric enzyme assay, brush border membrane vesicles were solubilized for 30 min at 4°C with 1% Doc in 50 mM Tris-HCl, pH 8.5, without protease inhibitors. Renal corpuscles were isolated from kidneys of young Balb/c mice as previously described (34). The kidneys were perfused with ferric oxide and subsequently pushed through a 90-μm pore size stainless steel sieve, after which the renal corpuscles were separated from other renal components with a magnet. The highly enriched renal corpuscle suspension, containing <5% tubule or vascular fragments, was solubilized in 1% Doc and used in the immunoprecipitation. A complete thymus from a young Balb/c mouse was solubilized in 1% Triton X-100. This preparation of solubilized thymic antigens was used in the immunoprecipitation technique. Protein concentrations were determined by the method of Lowry (35).

Monoclonal Antibodies to APA and DPP IV. Male Lou rats were immunized IP with the detergent phase of the Triton X-114 extract of mouse brush border preparation, as described (7). Spleen cells from the Lou rats were fused with SP 2/0 mouse myeloma cells by the procedure of Köhler and Milstein (36). Hybridomas were grown in 96-well tissue culture plates (Costar; Cambridge, MA) with HEPES-buffered RPMI-1640 culture medium (MA Bioproducts; Bethesda, MD), containing 10% decomplemented fetal calf serum, gentamicin (40 μg/ml), 1 mM L-glutamine, 1 mM sodium pyruvate, and 10% supernatant of a human umbilical vein cell culture, supplemented with HAT. Hybridomas were selected for production of antibodies to antigens present on both brush border membrane and podocytes by indirect immunofluorescence (IF) on acetone-fixed cryostat sections from normal mouse kidneys. Selected hybridomas were cloned several times by limiting dilution until all subclones showed the same reactivity pattern in the indirect IF screening procedure. Ascites containing MAbs was subsequently produced in Balb/c, nu/nu mice, and was purified by ammonium sulfate precipitation. The MAbs coded ASD-4 and ASD-36 were selected for this study. The IgG content of the MAb preparations was measured by radial immunodiffusion (37). IgG subclasses were determined with an isotyping kit for rat MAbs according to the instructions of the manufacturer (Serotec; Oxford, UK). The test system is based on rat cell agglutination with highly specific antibodies directed to isotypes of rat IgG attached to sheep erythrocytes (38).

Immunoprecipitation. By a solid-phase immunoprecipitation procedure (39), APA and DPP IV were isolated from suspensions of detergent solubilized renal corpuscles (1% Doc), brush border vesicles (1% Doc), and thymus (1% Triton X-100) and were analyzed by SDS-PAGE. All three fractions were radiolabeled with ^{125}I (Amersham; Buckinghamshire, UK) using iodobeads (Pierce Chemical; Rockford, IL) as a coupling reagent (40). Free ^{125}I was removed by Sephadex G-25 chromatography. Polystyrene microtiter plates (Costar) were precoated with 10 μg/well affinity-purified goat anti-rat Ig antibodies (Cappel–Organon Teknika; Boxtel, The Netherlands) in PBS for 18 h at 4°C. After five washes with PBS containing 0.05% Tween, the wells were coated with 100 μl/well of purified ascites containing 10 mg Ig/ml of MAb for 3 hr at 37°C. After five further washes the wells were blocked for 3 hr at 21°C with PBS containing 1% BSA and 1% normal rat serum, and then again washed five times. The wells were next incubated for 2 hr at 21°C with the ^{125}I-labeled kidney or thymic suspensions. The wells were then washed 10 times with immunoprecipitation (IP) buffer (150 mM NaCl, 50 mM Tris, 5 mM EDTA, 0.1% Triton X-100, 0.02% SDS, 10 U/ml Trasylol, 1 mM PMSF, and 1 mM benzamidine; pH 7.4). Next, 100 μl/well of reducing (2.3% SDS, 200 mM dithiothreitol, 10% glycerol, 60 mM Tris-HCl, pH 6.8) or nonreducing (2.3% SDS, 10% glycerol, 60 mM Tris-HCl, pH 6.8) SDS sample buffer was added, after which the wells were incubated for 15 min at 60°C and then for 5 min at 100°C. The immunoisolated proteins were analyzed by SDS-PAGE in 7.5% acrylamide according to Laemmli (41). For autoradiography, the gels were dried and exposed at −70°C with preflashed X-ray film (Kodax X-Omat).

Fluorimetric Enzyme Assay. The specificity of ASD-4 for APA and ASD-36 for DPP IV was determined by a solid-phase immunodepletion procedure as described (7,42). The purified MAb was first coupled to cyanogen bromide-activated Sepharose 4B (S4B) according to the instructions of the manufacturer (Pharmacia; Uppsala, Sweden). Briefly, 5 mg of the selected MAb in 1 ml of 0.1 M carbonate buffer, pH 8.4, containing 0.5 M NaCl, was added per ml of S4B. Residual binding sites were saturated with 1 M ethanolamine. A brush border suspension solubilized in 1% Doc containing 4 mg protein was dissolved in 5 ml buffer (20 mM Tris-HCl, pH 8.4, containing 0.1% Doc) and was incubated for 17 hr at 4°C under constant stirring with 1 ml of S4B coupled with MAb. In a control experiment, a brush border solution was incubated with S4B beads to which no MAb had been coupled. The supernatant was removed and the beads were washed several times with buffer. Elution of the antigen bound to 1 ml of beads was performed with 5 ml of 50 mM diethylamine containing 0.1% sodium deoxycholate, pH 11.5, for 5 min. The eluted proteins were neutralized with 2 M Tris, pH 7.4. The enzymatic activities for APA, DPP IV, and APN were measured fluorimetrically in the control brush border–Doc solution, the immunodepleted solution, and the eluate, using L-glutamic acid-α-7-amido-4-methylcoumarin (Glu.AMC), glycyl-L-proline-7-amido-4-methylcoumarin-HBr (Gly.Pro.AMC; both from Bachem, Bubendorf, Switzerland), and L-alanine-7-amido-4-methylcourmarin (Ala.AMC; from Serva, Heidelberg, Germany) as specific and sensitive substrates for APA, DPP IV, and APN, respectively (43). For determination of APA activity, the three fractions and the substrates were solubilized in 0.1 M Tris-HCl buffer containing 1.25 mM $CaCl_2$, pH 7.0. For APN activity, 0.1 M Tris-HCL buffer, pH 7.0, and for DPP IV activity 0.1 M Tris-HCl buffer, pH 8.0, were used as solutions. Ten μl of one of the three fractions was incubated with 100 μl of one of the three substrates ($2 \cdot 10^{-4}$ M) for 20 min at 37°C. The reaction was stopped by addition of 890 μl of 0.2 M Tris-NaOH, pH 11. The enzyme activities were determined by the fluorescence of 7-amino-4-methylcoumarin cleaved from the substrates (43). The fluorescence was measured at 375 nm (excitation) and 440 nm (emission) using a luminescence spectrometer (LS5; Perkin Elmer, Norwalk, CT). The enzyme activities of the various fractions are expressed as nkatal/ml, 1 nkatal being the amount of enzyme that converts 1 nmol of substrate/sec under the given assay conditions, or as percentages of the activities present in the control brush border solution.

Indirect Immunofluorescence. Because in preliminary studies we had found no differences in the localization of both hydrolases between male and female mice, except for the reproductive organs, we present the localization found in male mice. Fragments of organs from a 2-month-old male Balb/c mouse, as listed in Table 1, were snap-frozen in liquid nitrogen. For indirect IF of the female reproductive organs, a 2-month-old female Balb/c mouse was used. Two µm-thick, acetone-fixed cryostat sections were incubated with MAbs ASD-4 and ASD-36 for 30 min at room temperature. Binding of the two MAbs to the various tissues was visualized with FITC-labeled goat anti-rat IgG containing 1.5% normal mouse serum (Cappel–Organon Teknika). We differentiated in some organs the presence of both hydrolases from B-cells or endothelial cells by additional double labeling experiments in which incubation of ASD-4 or ASD-36 was followed by incubation of TRITC-labeled goat anti-mouse Ig for identification of B-cells or of the TRITC-conjugated lectin *Griffonia simplicifolia* (Sanbio; Uden, The Netherlands), which identifies specifically mouse endothelial cells (44). To define more precisely in the thymus the presence of APA, sections were double labeled with ASD-4 (APA) and a mouse MAb to cytokeratin 2/8 (RCK 102) (45). The thymic sections were first incubated with ASD-4 diluted 1:100 in PBS/1% BSA, washed, and incubated with FITC-labeled goat anti-rat IgG diluted 1:25. After this binding the sections were preincubated with rabbit anti-mouse IgG diluted 1:100 in PBS/1% BSA, followed by a short wash in PBS. The sections were then incubated with an MAb against cytokeratin and washed again in PBS. TRITC-labeled rabbit anti-mouse IgG (ITK Diagnostics; Uithoorn, The Netherlands) was diluted 1:100 in PBS/1% BSA, and washed in PBS. All sections were embedded in Aquamount (BDH Chemicals, Poole, UK), and examined in a fluorescence microscope equipped with Ploemopak Epi-illumination (Leitz; Wetzlar, Germany). The staining intensity was recorded semiquantitatively on a scale from 0 to 4+, as described previously (9).

Enzyme Histochemistry. To correlate the localization of APA and DPP IV protein in the kidney and thymus with their enzymatic activities, we examined the enzymatic activities with specific substrates by the enzyme histochemistry technique. For enzyme histochemistry, a kidney and a thymus from a young Balb/c mouse were removed and snap-frozen in liquid nitrogen. For demonstration of APA and DPP IV activity, 5 µm-thick, acetone-fixed sections were incubated for 10 min for the kidney and for 30–45 min for the thymus at 37°C in substrate buffer containing 100 mM Tris-HCl, pH 7.0, 2 mM $CaCl_2$, 1.1 mM Fast Blue salt (Serva) 1.6 mM L-glutamic acid-α-methoxy-β-naphtylamide for APA, or 1.6 mM glycyl-L-proline-α-methoxy-β-naphtylamide for DPP IV (Bachem). After rinsing with PBS, the sections were embedded in Aquamount and examined by conventional light microscopy.

Immunoelectron Microscopy. The localization of APA and DPP IV in a restricted number of organs, i.e., kidney, liver, small intestine, thymus, and lung of a normal Balb/c mouse, was examined by indirect immunoelectron microscopy (IEM) using immunoperoxidase labeling on 20-µm frozen sections. A Balb/c mouse was first perfused retrogradely via the aorta with PBS for 5 min and subsequently with a mixture of 10 mM periodate, 75 mM lysine, and 2% paraformaldehyde, pH 6.2 (PLP) for 10 min (6). The organs selected for IEM were removed and small pieces were further fixed by immersion for an additional 3 hr in PLP. After rinsing several times in PBS, the fragments were cryoprotected by immersion in 2.3 M sucrose, pH 7.2, for 1 hr, and then frozen in liquid nitrogen. Twenty µm-thick sections were rinsed in PBS for 1 hr, then incubated with MAbs ASD-4 and ASD-36 diluted in PBS containing 1% BSA for 18 hr at 4°C, followed, after several washes with PBS, by incubation for 1.5 hr with a peroxidase-labeled rabbit anti-rat IgG diluted in PBS containing 1% BSA and 2% normal mouse serum. After three washes in PBS, the sections were incubated in PBS, pH 7.4, containing diaminobenzidine (DAB) medium for 10 min, followed by DAB with addition of 0.003% H_2O_2 for 7 min. The sections were washed in distilled water, postfixed in palade buffer containing 1% OsO_4 for 30 min at 4°C, dehydrated, and embedded in Epon 812. Thin sections were prepared on a LKB ultratome (LKB Instruments; Bromma, Sweden) and examined by electron microscopy (JEOL 1200 EX2; JEOL, Tokyo, Japan).

Results

Characterization of the MAbs

The two rat MAbs that were selected for this study, ASD-4 and ASD-36, were of the IgG_1 and IgG_{2b} subclass, respectively (7). The molecular weights of the antigens isolated by the MABs in the solid phase immunoisolation technique on radiolabeled preparations of renal corpuscles, renal brush borders (Figure 1), and thymus (Figure 2) were determined by SDS-PAGE under reducing conditions. ASD-4 precipitated a protein of 140 KD from both renal brush borders (Figure 1, Lane 1) and thymus (Figure 2, Lane 1), representing the monomeric form of APA as described earlier (23,24,46). The monomeric APA protein in renal corpuscles had a higher molecular weight of 163 KD (Figure 1, Lane 2). A high molecular weight protein of more than 200 KD was also seen in renal corpuscles and renal brush borders (Figure 1, Lanes 1 and 2), and thymus (Figure 2, Lane 1), representing the intact homodimer of APA that resisted the reducing conditions as described previously (23). ASD-36 isolated a protein of 116 KD from both renal corpuscles (Figure 1, Lane 5) and thymus (Figure 2, Lane 2), representing the monomeric DPP IV form (23). The monomeric DPP IV form from renal brush borders had a lower molecular weight of 103 KD (Figure 1, Lane 4). In control experiments using normal rat serum instead of MAbs no proteins were isolated from the radiolabeled renal corpuscles and renal brush borders (Figure 1, Lanes 3 and 6). An additional low molecular weight-protein of 43 KD was precipitated by both ASD-4 and ASD-36 from the thymus (Figure 2, Lane 2), renal corpuscles, and renal brush borders (data not shown). The protein recognized by ASD-36 is most probably the enzyme adenosine deaminase (47), and the band isolated by ASD-4 is actin that co-precipitated with APA (48). These immunoprecipitation experiments show that there are differences in molecular weight of APA as well as DPP IV from different organs (kidney vs thymus), and from different structures within the same organ (renal corpuscles vs brush borders).

Specificity of the MAbs

The specificity of the MAbs for the brush border hydrolases APA and DPP IV was determined by an immunoadsorption procedure using Sepharose-4B beads coated with either ASD-4 or ASD-36 MAb. Enzymatic activities for APA, DPP IV, and aminopeptidase N (APN; EC 3.4.11.2) detected in the sodium deoxycholate (Doc) solubilized brush border fraction using specific substrates in the fluorimetric assay were 5.3, 17.1, and 50.7 nkatal, respectively. The APA activity was selectively depleted from the brush border–Doc solution by ASD-4 (3%), whereas DPP IV activity was selectively depleted by ASD-36 (3%) (Figures 3A and B). In both cases, the activities for the other two enzymes remained unaltered. Subse-

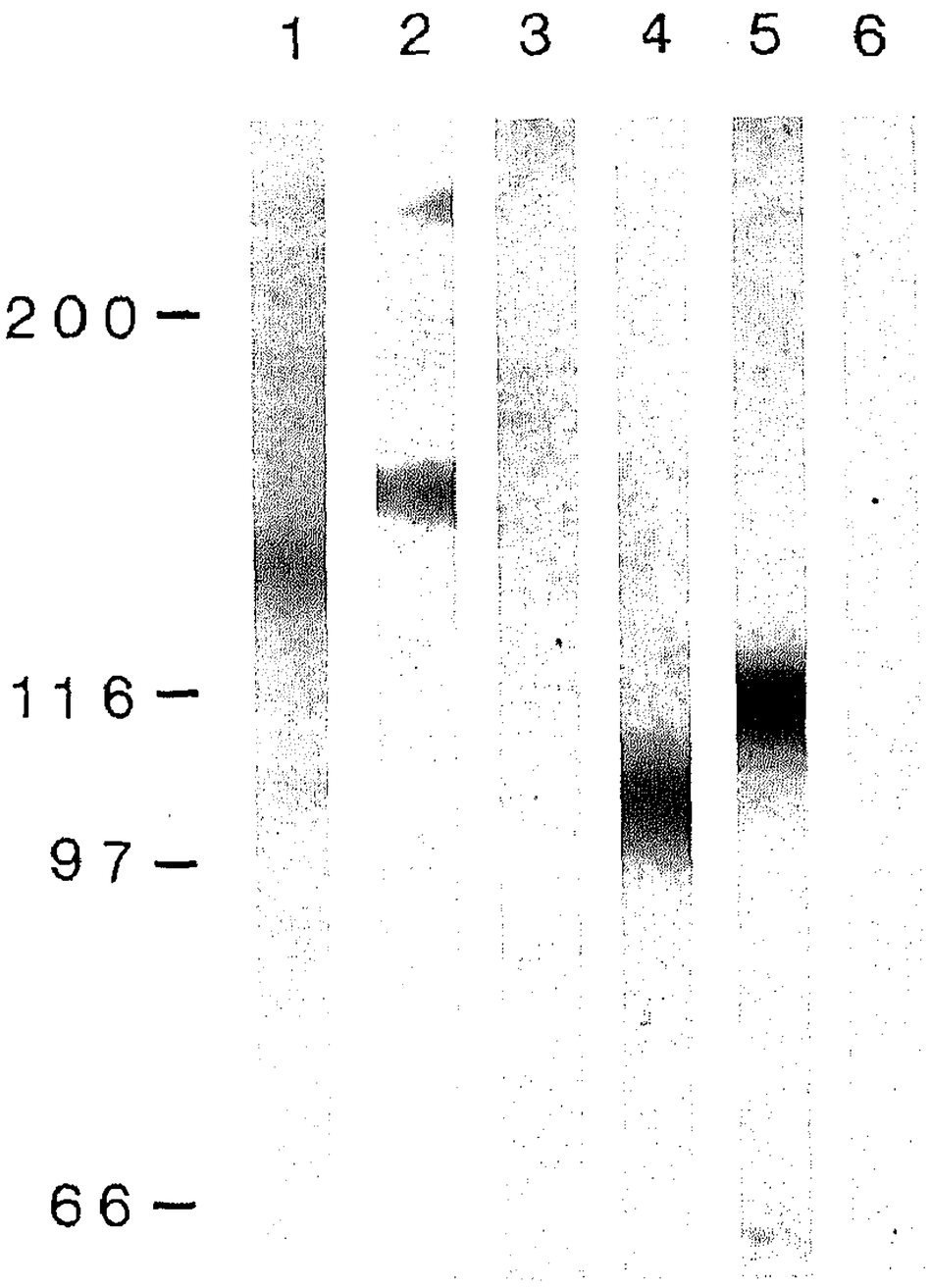

Figure 1. Autoradiogram of the immunoprecipitation analysis of radiolabeled suspensions of mouse renal brush orders (Lanes 1, 3, 4, and 6), and renal corpuscles (Lanes 2 and 5) after SDS-PAGE (10%) under reducing conditions. Lanes 1 and 2 (ASD-4), a rat MAb against mouse APA; Lanes 4 and 5 (ASD-36), a rat MAb against mouse DPP IV; Lanes 3 and 6, normal rat serum. Numbers at left indicate the molecular mass of the markers.

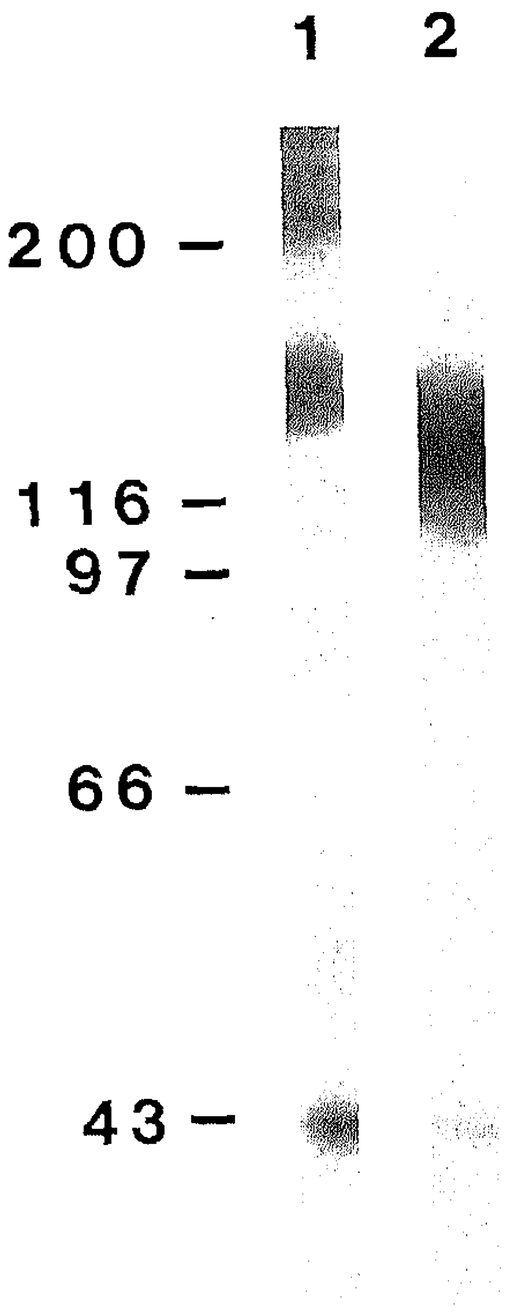

Figure 2. Autoradiogram of the immunopreciptation analysis of radiolabeled proteins from mouse thymus after SDS-PAGE (10%) under reducing conditions. Lane 1 (ASD-4), a rat MAb against mouse APA; Lane 2 (ASD-36), a rat MAb against mouse DPP IV. Numbers at left indicate the molecular mass of the markers.

quently, absorbed enzyme could be recovered from the column by elution. The low reactivity of the eluates (25% for APA and 30% for DPP IV) is probably due to inactivation of the enzyme caused by the elution procedure. The selective depletion of APA activity by ASD-4 and of DPP IV activity by ASD-36 indicates that ASD-4 is directed against APA and ASD-36 is directed against DPP IV.

Organ Distribution of APA and DPP IV

By indirect IF and IEM, both APA and DPP IV showed a widespread organ distribution, as summarized in Table 1. In some organs the two enzymes were located on the same cells, such as in the cortex of the kidney (Figures 4A and B), small intestine (Figures 10A and 10B), liver (Figures 10E and 10F), various glands, visceral yolk sac of the placenta, choroid plexus of the eye (Figure 12F), and perineurium. In other organs the enzymes were present in separate segments of the same epithelium, such as in the uterus, with DPP IV predominantly being localized on the inner lining of the uterus and APA more on the ductal side of the epithelium (Figures 12I and 12J). On the other hand, APA and DPP IV were present on separate cells in the thymus (Figures 8 and 9), brain (Figures 12A and 12B), and spleen and lymph nodes (Figures 12C and 12D). In contrast to DPP IV, APA was also found in almost all organs on the endothelial cells of capillaries (Figures 4C, 5C, 10C, and 12A), but not of arteries and veins, although sometimes a heterogeneous distribution was seen, such as in the kidney (Figures 4A and 4C). In addition, APA could be found on smooth muscle cells of the media of arterioles (Figure 12C). DPP IV, however, was present on cells of serosal cavities (Figure 11D), cells in fibrous capsules around many organs, and astrocytes in cerebrum and spinal cord (Figure 12B).

In the kidney, APA and DPP IV are co-expressed mainly on identical cells in the cortex, but not in the medulla. In the glomerulus, both enzymes are located on the cell membranes of the podocytes, but not on the endothelial or messangial cells as seen by indirect IF and IEM (Figures 4A, 4B, 5A, and 6A). The enzymes were also present on the brush borders of the proximal tubule cells, i.e., APA predominantly on the convoluted parts (S1 and S2), whereas DPP IV was present along the entire proximal tubule (Figures 4A, 4B, 5B, and 6B). In contrast to DPP IV, APA was observed on the juxtaglomerular granular cells, the cells of the arteriolar media, and endothelial cells of the peritubular capillaries, especially of the

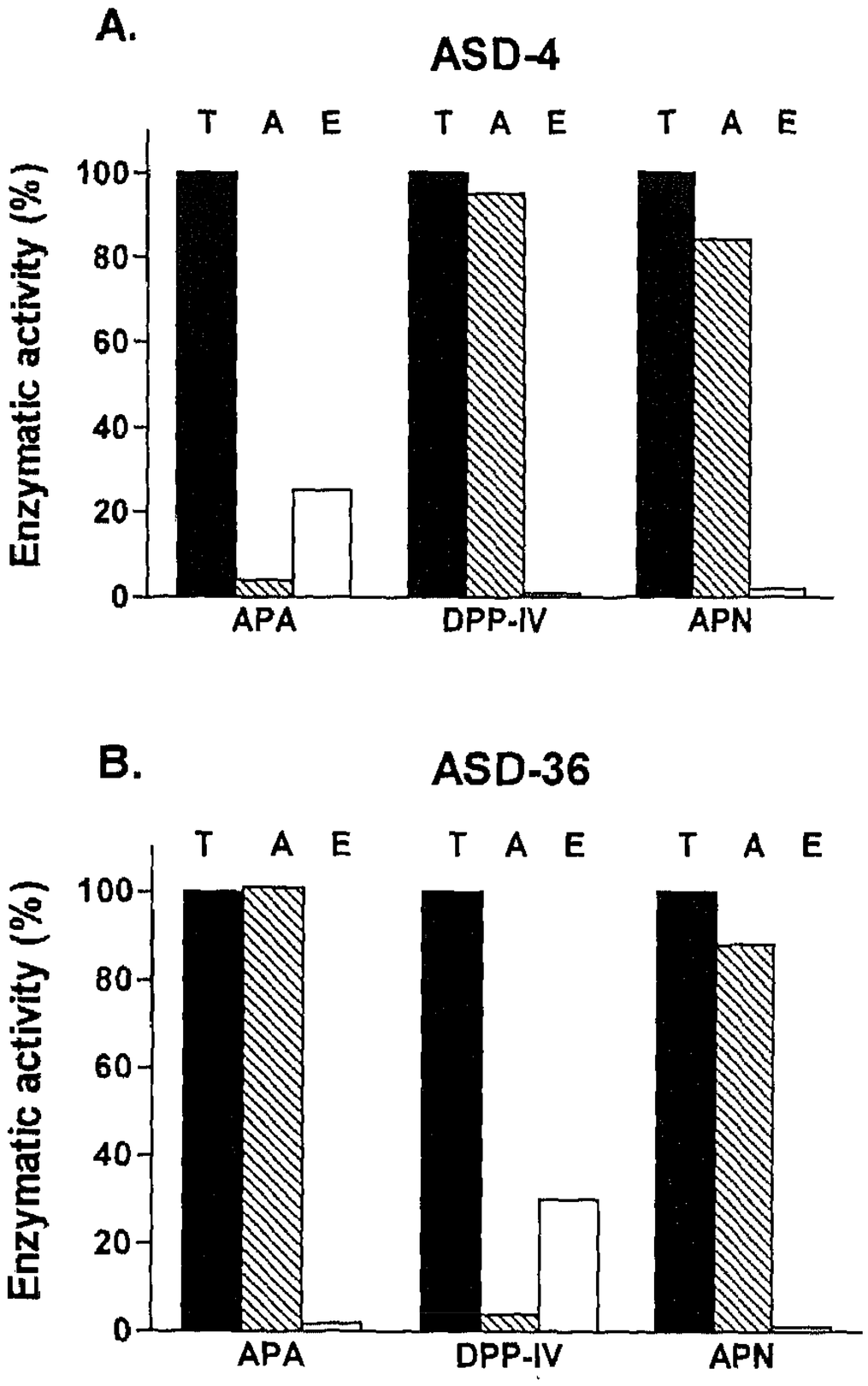

Figure 3. Enzymatic activities of APA, DPP IV, and APN measured in two immunodepletion experiments with ASD-4, an MAb against APA **(A)** and ASD-36, an MAb against DPP IV **(B)** in three fractions using a fluorimetric enzyme assay. A detergent-solubilized brush border fraction (T, black bars), a brush border fraction immunodepleted with ASD-4 or ASD-36 coupled to Sepharose-4B beads (A, hatched bars), and a fraction eluted from the beads (E, open bars). The enzymatic activities are given as percentages of the activities in the starting material (100%).

medulla (Figures 4C and 5B). DPP IV, on the other hand, was found on the cells of Henle's loops, as demonstrated by a double labeling IF procedure and by IEM (Figures 4D and 6C). The localization of APA and DPP IV, as revealed by immunohistology with ASD-4 and ASD-36, respectively, matched the enzymatic activities as demonstrated by enzyme histochemistry using specific substrates (Figure 7).

In contrast to the co-localization of APA and DPP IV in the kidney, there was clearly a different expression of the two hydrolases on cells in the thymus, spleen, and lymph nodes, suggesting different functions related to the development of thymocytes and activation of the T-cells (Figures 8, 12C, and 12D). APA was expressed only on cortical epithelial cells of the thymus, as confirmed in a double labeling experiment with an MAb specific for cytokeratin 2/8, which is present only on thymic epithelial cells (Figures 8A and 8B). APA expression, as demonstrated by ASD-4, and its enzymatic activity, as shown by enzyme histochemistry, matched each other and were both found on cortical epithelial cells (Figures 8C, and 8D). APA was not present on cells in the medulla (Figure 8A). DPP IV was present on cells in the medulla (Figure 8A). DPP IV was present on thymocytes, as shown by immunohistological staining with ASD-36 and enzyme histochemistry (Figures 8E and 8F). The expression of DPP IV varied from cortex to medulla, with higher expression in the thymic cortex, corresponding to earlier reports (49). IEM with ASD-4 showed staining of the cell membranes of the cortical epithelial cells with its finger-like cell protrusions interdigitating between surrounding thymocytes (Figure 9A). ASD-36 stained all thymocytes, as shown in Figure 9B. In the peripheral lymphoid organs, DPP IV was found on T-cells and not on B-cells, as examined by double labeling with antibodies to IgM. In the spleen these T-cells were located around arterioles, which showed the presence of APA on the smooth muscle cells (Figures 12C and 12D).

Both APA and DPP IV were abundantly co-expressed on the brush borders of the small intestine, which diffusely stained with ASD-4 and ASD-36, respectively, by indirect IF (Figures 10A and 10B), and IEM (Figure 11C). The same co-expression was observed in the liver, in which APA and DPP IV were present in various amounts on sinusoidal lining cells, bile canaliculi and, to a lesser extent, on hepatocytes (Figures 10E and 10F). Their localization was more clearly demonstrated by indirect IEM (Figures 11A and 11B). In the lung, as in most other organs, APA was present on the endothelial cells of the alveolar walls. In addition, it could be seen on the large Type II alveolar cells, but not on the smaller Type I alveolar cells (Figures 10C and 11E). DPP IV was mainly located on Type I cells (Figures 10D and 11F). In the brain and spinal cord, APA was present only on endothelial cells of the capillaries, whereas DPP IV was shown on astrocytes (Figures 12A and 12B). Prominent staining with ASD-4 was also seen on follicle cells of the ovary and, to a lesser extent, on the cornea (Figures 12K and 12E). Finally, DPP IV could be found on cells of the islets of Langerhans (Figure 12H), the epithelium of the Harderian gland of the eye, and the germinal epithelium of the ovary.

Discussion

This study examined the presence of two important hydrolases, APA and DPP IV, in organs of the mouse. This pattern of localization might enable us to provide more insight into the various biological functions that are attributed to them. APA and DPP IV are well-known differentiation markers of lymphoid and myeloid progenitors and are believed to participate in stromal cell-dependent B- and T-cell differentiation and in T-cell activation (23,24,50). In general, two ill-defined processes are related to the functions of these two enzymes. First, both hydrolases are involved in degradation and uptake of peptides by epithelial cells, such as the cells of the renal proximal tubules and the small intestine. Second, by breaking down ligands such as peptide hormones, growth factors, cytokines, or other regulatory proteins involved in cell activation, growth, and differentiation, APA and DPP IV can reduce or limit the cellular response induced by these ligands. It is in this second field that some progress has been made in recent years.

APA is a disulfide-linked homodimer that could easily be im-

Table 1. *Organ distribution of APA and DPP IV*[a]

Organ	Distribution		APA	DPP IV
Kidney	Glomerulus		+ + +	+ + +
	Proximal tubules BB microvilli	S1	+ + +	+ +
		S2	+ + +	+ +
		S3	+	+ +
	Distal tubules		−	−
	Loops of Henle		−	+
	Peritubular capillaries		+ / + +	−
	Pars media arteries		+ +	−
	Juxtaglomerular granular cells		+	−
	Capsule		−	+ +
Prostate	Epithelium		−	+ +
Vesicular gland	Epithelium		−	+
Epididymis	Epithelium		±	+ / + +
Vas deferens	Epithelium		−	+ / + +
Ovary	Germinal epithelium		−	+ + / + + +
	Folicle cells		+ + +	−
Oviduct	Epithelium		− / ±	+ +
Uterus	Epithelium		− / ±	+ + +
	Crypt epithelium		+ / + +	+ + +
Placenta	Visceral yolk sac		+ +	+ +
Tongue	Serous glands		+ +	+ +
Small intestine	Duodenum BB microvilli		+ + + +	+ +
	Jejunum BB microvilli		+ + + +	+ + +
	Ileum BB microvilli		+ + + +	+ + +
Large intestine	Epithelium		− / ±	+
Liver	Sinusoidal lining cells		+ +	+ +
	Hepatocytes		+	+
	Bile canaliculus		+ +	+ + + +
	Bile duct		+	+
Gallbladder	Epithelium		+ / + +	− / ±
Trachea	Serous glands		+	+
Lung	Alveolar wall			
	Endothelium		+ + +	−
	Alveolar cell Type I		−	+ +
	Alveolar cell Type II		+ + +	+
Pituitary gland	Intermediate lobe		+	−
Adrenal gland	Cortex, sinuses		+ + +	−
Salivary glands				
Parotid	Epithelium		+ +	+ + +
Submandibular	Epithelium		−	+ +
Sublingual	Epithelium		−	+ +
Pancreas	Islets of Langerhans		±	+ +
	Epithelium of small ducts		+	+ + +
Thymus	Thymocytes (T-cells)		−	+ +
	Cortical epithelial cells		+ +	−
Spleen	Lymphocytes (T-cells)		−	+ +
Lymph node	Lymphocytes (T-cells)		−	+ +
	Sinuses		+	−
Skin	Hair follicle (basis)		+ +	+ +
Eye	Cornea		+	−
	Iris		±	+
	Ciliary body		±	+
	Choroid		+ + +	+ +
	Harderian gland		−	+
	Lacrimal gland		+ + +	+ + +
Cerebrum	Cortical astrocytes		−	+ + +
Cerebellum	Pia mater		−	+
Spinal cord	Astrocytes		−	+ +
Nerves	Perineurium		+ +	+ +
Smooth muscle	Pars media arteries		+ +	−
Multiorgan	Capillary endothelium		+ +	−
	Serosal layer		−	+ + +
	Capsule cells		−	+ + +
	Fibroblasts		+	+

[a] BB, brush border.

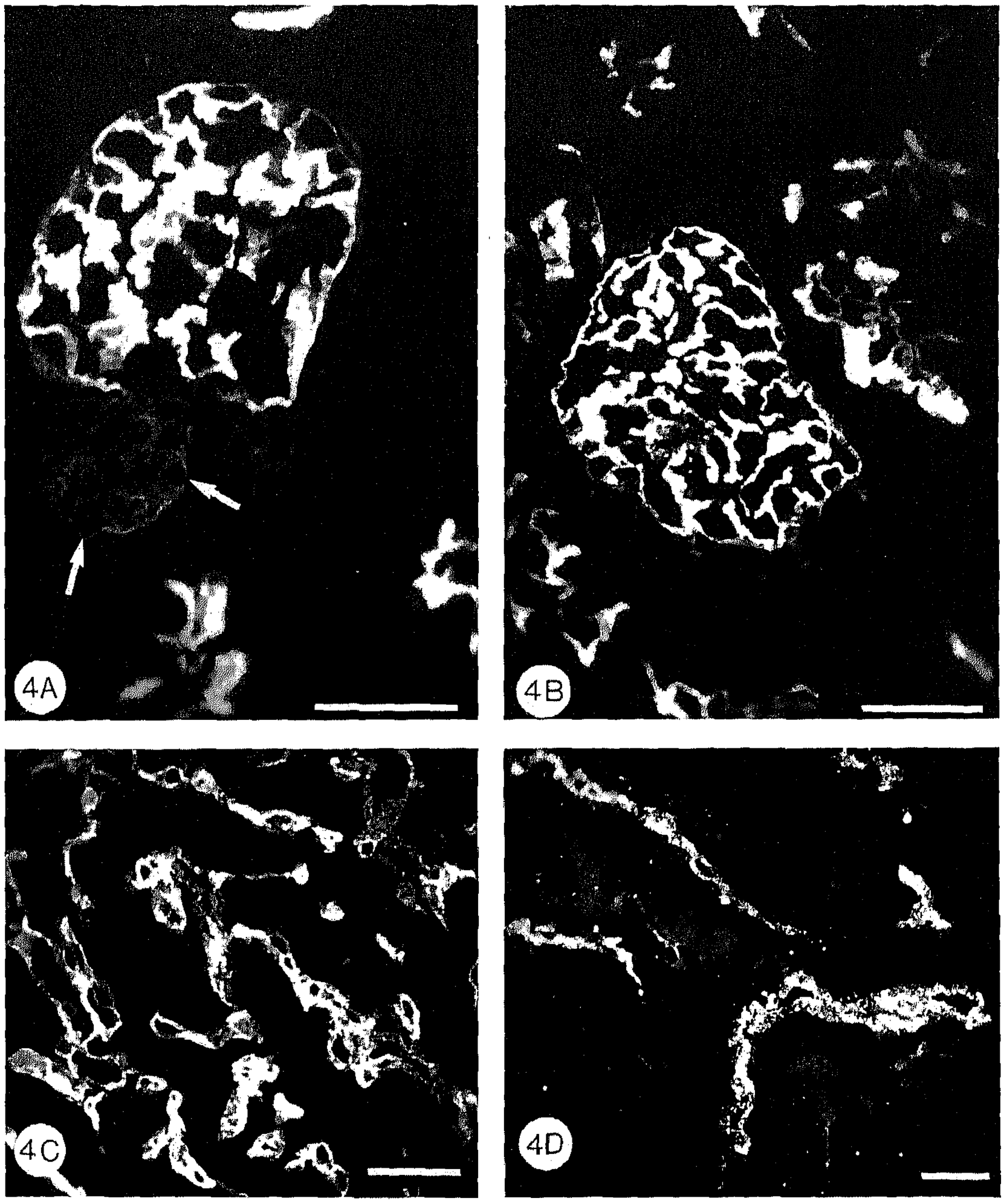

Figure 4. Indirect immunofluorescence of a normal Balb/c kidney incubated with ASD-4 **(A,C)**, and ASD-36 **(B,D)**. **(A)** Incubation with ASD-4 caused strong homogeneous binding along the capillary wall of the glomerulus and the brush borders of the proximal tubules. In addition, a faint granular staining of the juxtaglomerular granular cells is present (arrows). **(C)** In the medulla, ASD-4 bound strongly to the endothelial cells of the peritubular capillaries. **(B)** ASD-36 also strongly stained the glomerular capillary wall and the brush borders of the proxima tubules. **(D)** In the medulla, ASD-36 did not stain the endothelial cells of the capillaries, but the cells of Henle's loops were positive as detected with a double labeling technique using a lectin specific for mouse endothelial cells. *Original magnifications*: **A** × 850; **B** × 700; **C** × 550; **D** × 400. Bars = 25 μm.

munoprecipitated from the kidney and the thymus by ASD-4. The different molecular weights of APA isolated in this study from renal corpuscles, renal brush borders of proximal tubule epithelial cells, and thymus are not the products of different APA isoforms but probably reflect differences in glycosylation. Several arguments support this presumption. First, the isolated mouse cDNA sequence predicts a Type II, 945-amino-acid, integral cell membrane-bound protein of about 108 KD with a large extracellular domain, containing nine possible N-glycosylation sites (51). Second, incubation of APA with glycolytic enzymes also yielded an identical protein backbone of almost 110 KD (52) (personal observation). Third, Northern blotting experiments on poly A^+ RNA from different mouse organs always showed a single hybridizing band of approximately 4 KB (28). APA has a short-18-amino-acid cytoplasmic tail that is covalently coupled to actin, as reported by us (48,51), indicating a role of actin in the transport of APA in various cells. APA digests N-terminal glutamyl and aspartyl residues from peptides (53). APA that is expressed on early B-cells and on stromal cells in the bone marrow has an incompletely defined function in early B-cell development (51,54,55). One of the best known functions of APA is its regulatory effect on the renin–angiotensin system, since APA converts angiotensin II, the most active component of this system, into angiotensin III by removal of the N-terminal aspartyl residue (56). Angiotensin II has several effects on the cardiovascular system by its vasopressor and growth-promoting actions. The hemodynamic effects in the kidney are related to its regulatory role of the renal blood flow, glomerular filtration rate, sodium reabsorption in the proximal tubules, and induction of cell growth and hypertrophy of epithelial and muscle cells (57). All of these effects are mediated by its binding to several receptors (58,59). It has been

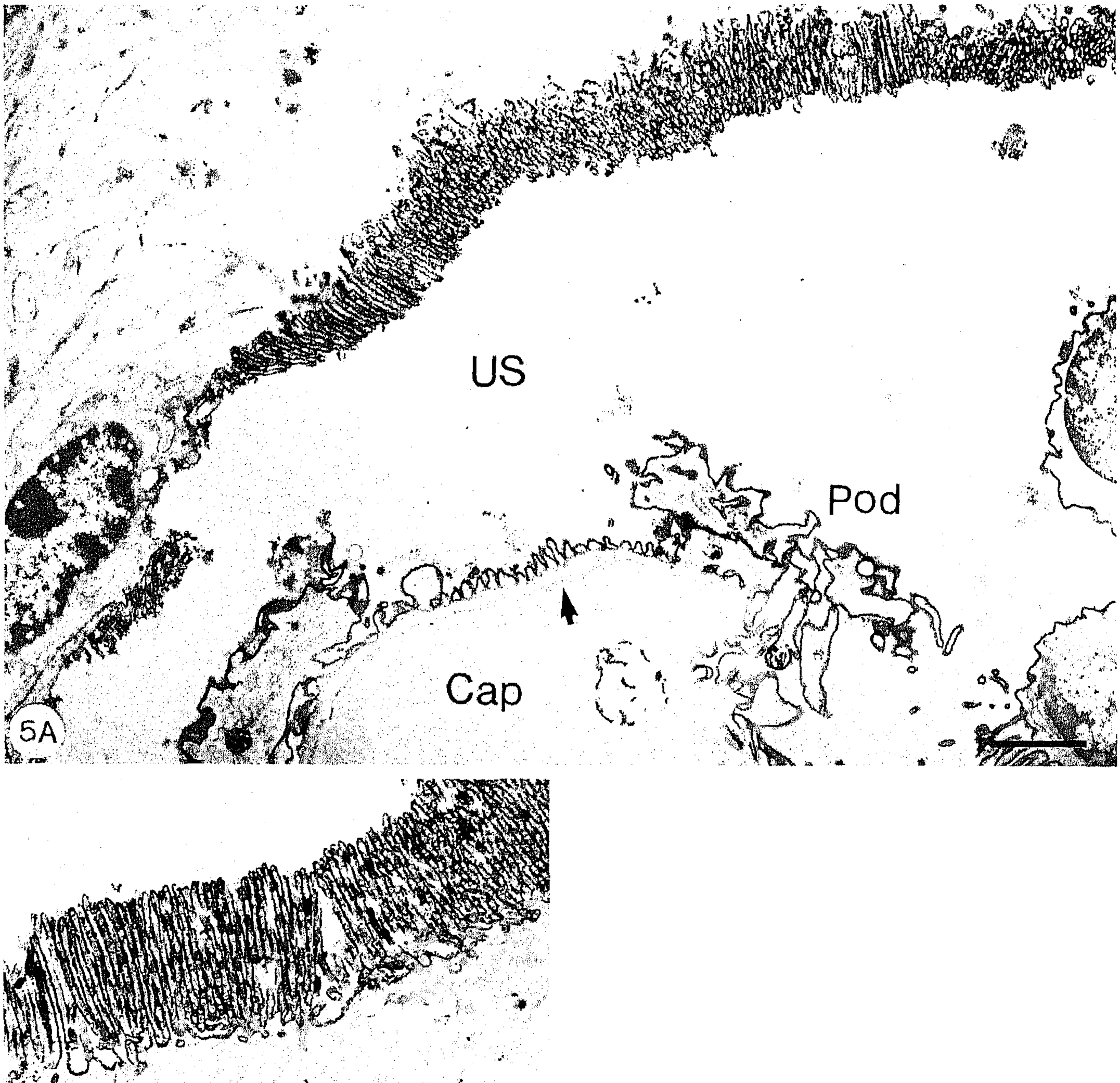

Figure 5. Indirect immunoelectron microscopy of a normal Balb/c kidney incubated with ASD-4, immunoperoxidase labeling. **(A)** Homogeneous staining of the cell membranes of the podocyte and the brush borders of the parietal epithelial cell is seen. The glomerular endothelial cell is negative (arrow). Cap, capillary lumen; Pod, podocyte; US, urinary space. **(B)** Proximal epithelial cell with staining of the brush borders. The endothelial cell of the peritubular capillary adjacent to the proximal tubule cell also shows faint staining (arrow). Original magnifications: **A** × 7000; **B** × 9500. Bars = 2 μm.

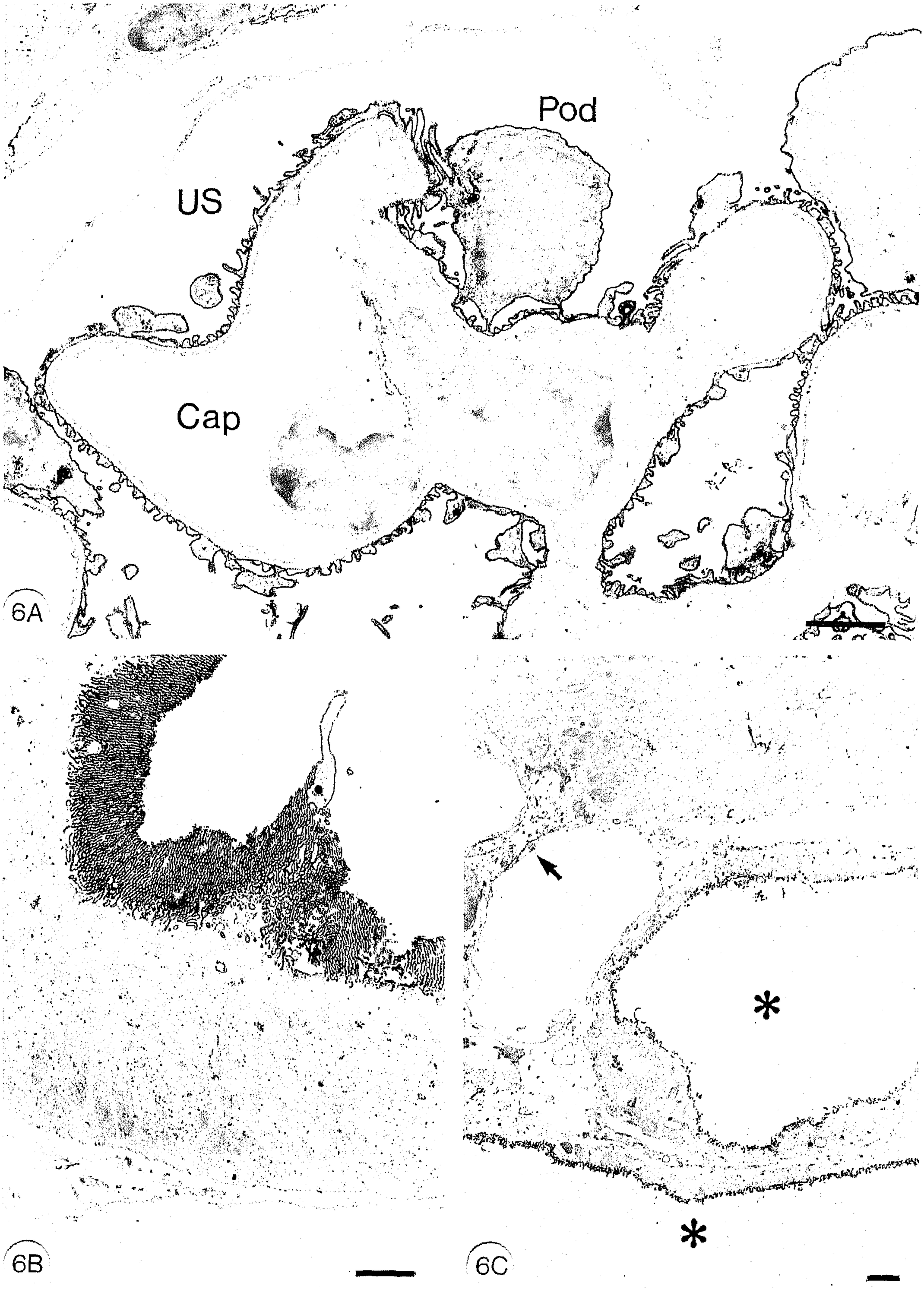

Figure 6. Indirect immunoelectron microscopy of a normal Balb/c kidney incubated with ASD-36, immunoperoxidase labeling. **(A)** Diffuse staining of the cell membranes of the podocyte. Glomerular endothelial and mesangial cells are negative. Cap, capillary lumen; Pod, podocyte; US, urinary space **(B)** Proximal tubule cell with homogeneous staining of the brush borders. The endothelial cell of the adjacent capillary is negative. **(C)** Medulla: homogeneous staining of the cell membranes of Henle's loops (asterisks). The endothelial cell (arrow) is negative. Original magnifications: **A** × 6700; **B** × 5000; **C** × 2700. Bars = 2 μm.

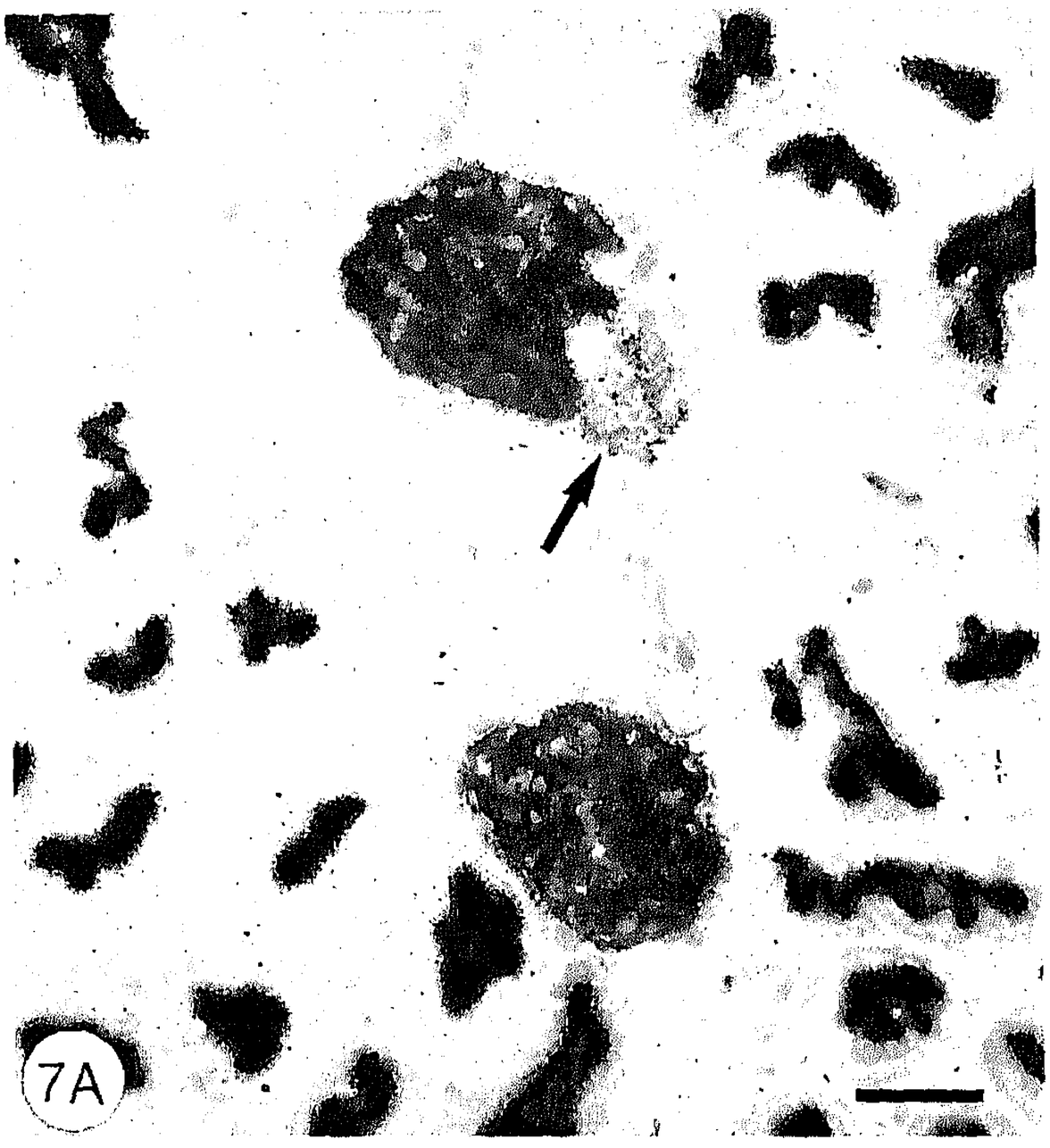

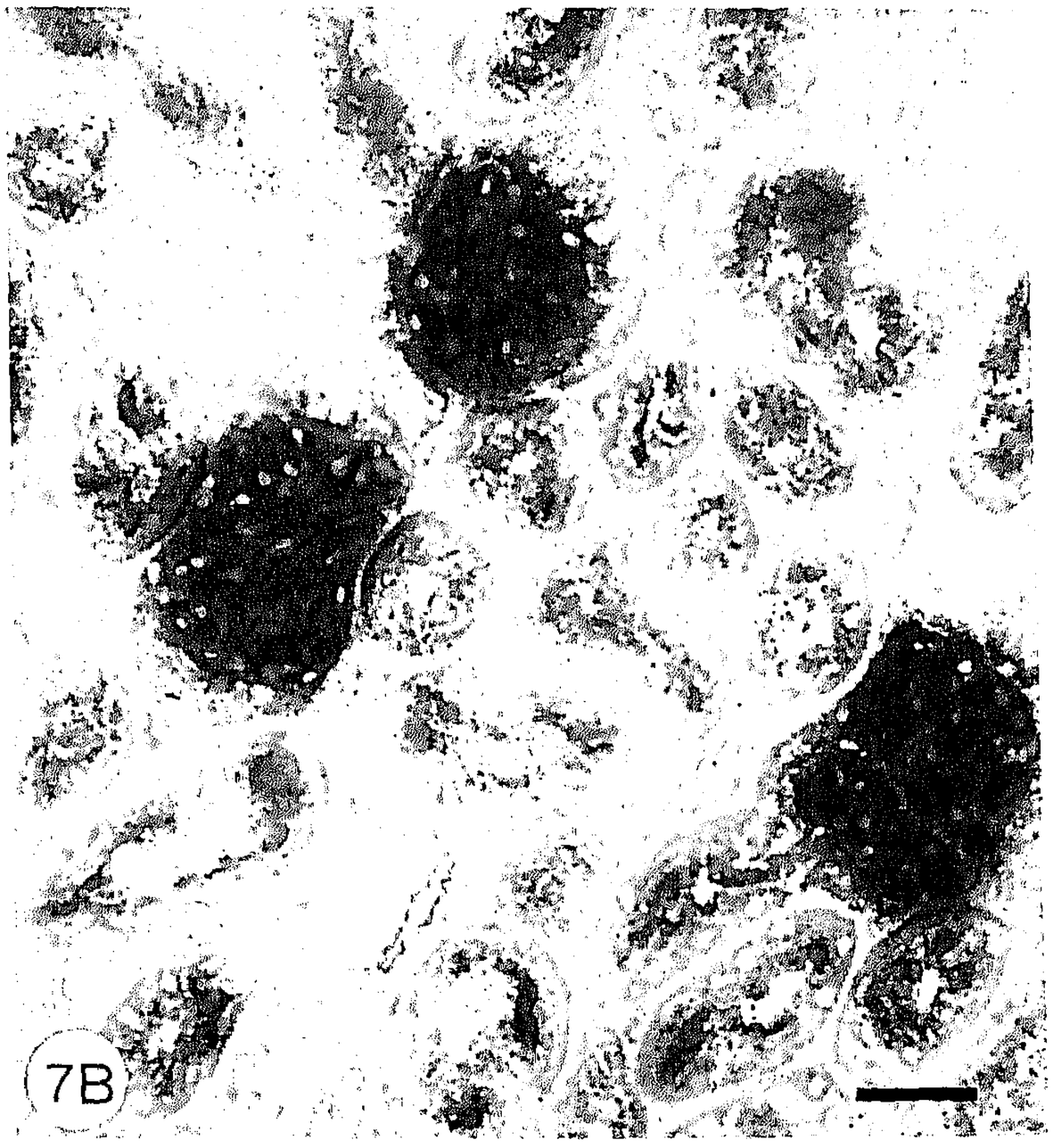

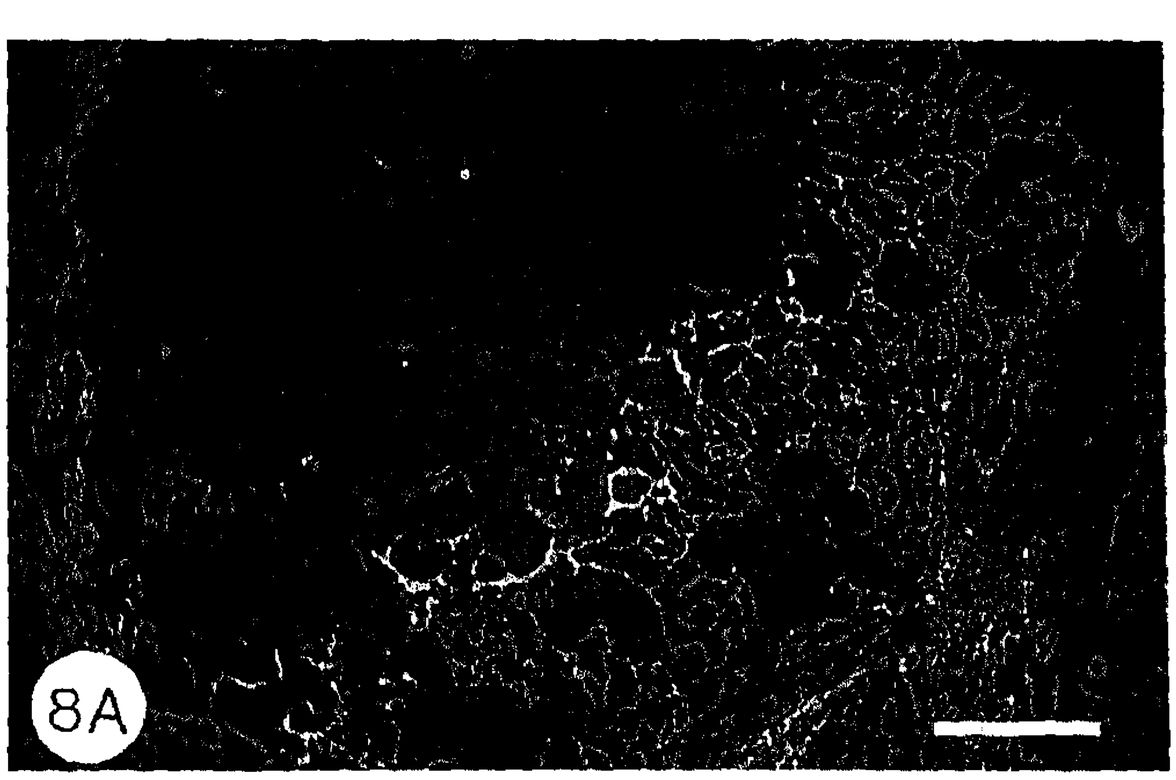

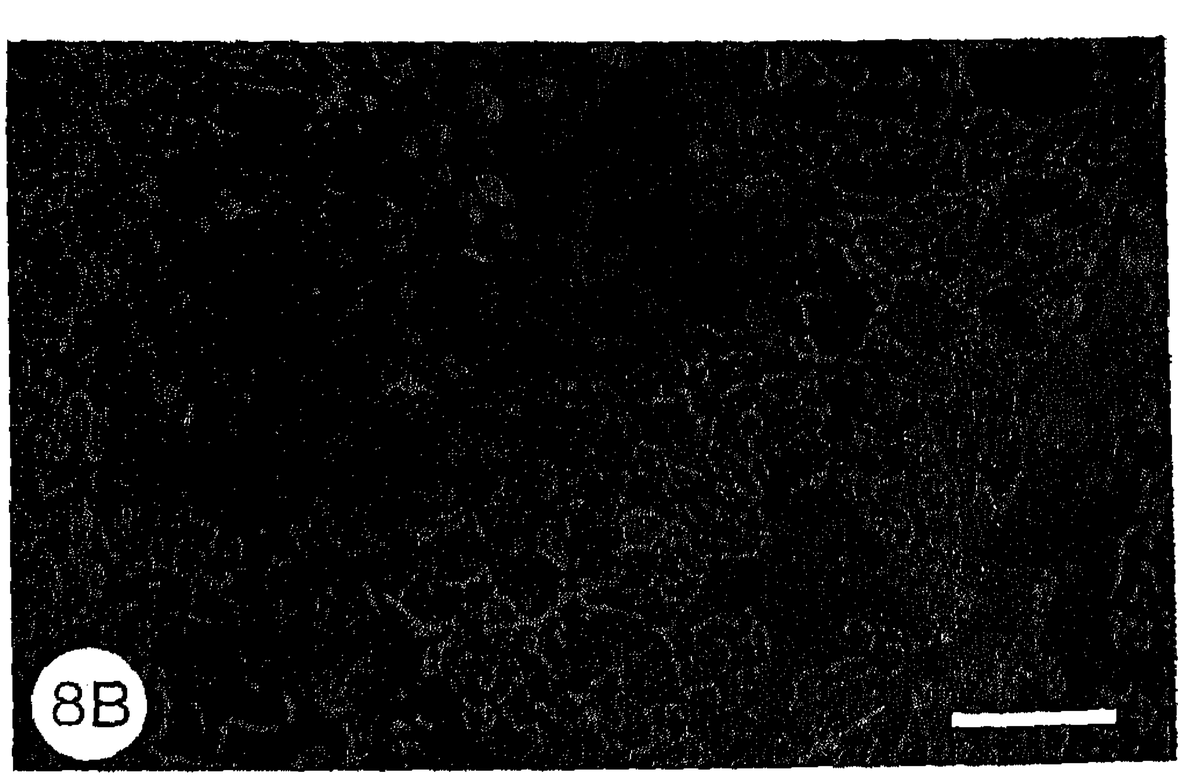

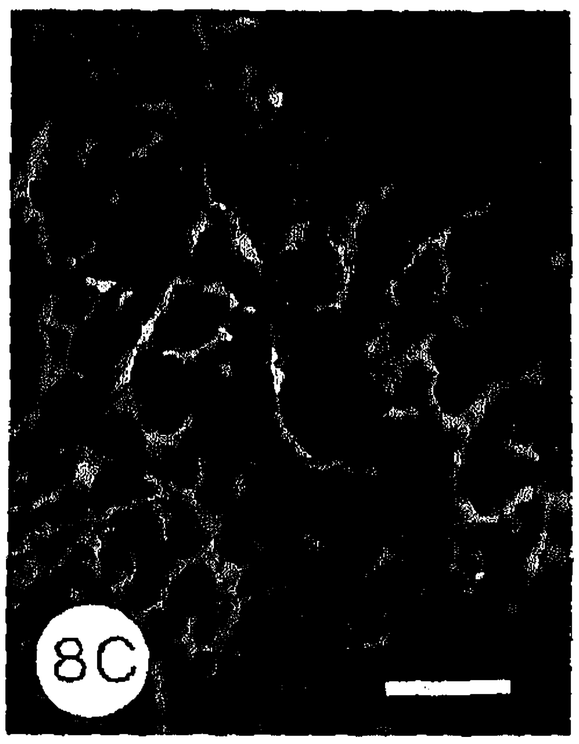

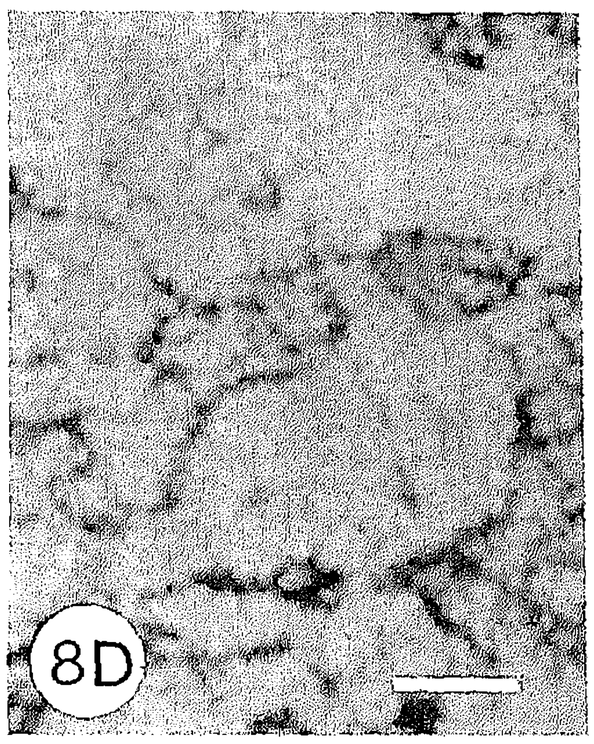

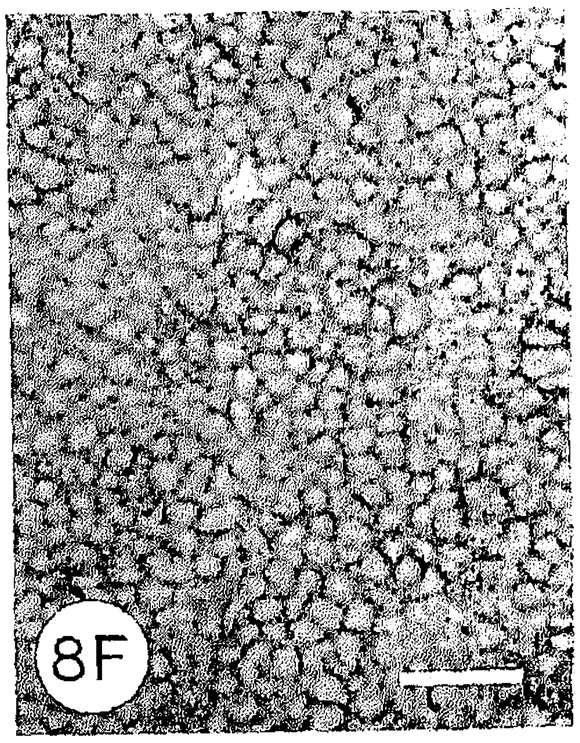

Figure 7. Enzyme histochemistry of a normal Balb/c kidney. **(A)** Incubation with an APA-specific substate shows strong staining of the brush borders of the proximal tubules and, to a lesser extent, of the glomerulus. Faint staining is seen in the juxtaglomerular granular cells (arrow). The staining of the peritubular capillaries, seen in immunohistology, is less obvious. **(B)** Incubation with a DPP IV-specific substrate shows strong staining of the glomerulus and moderate staining of the brush borders of the proximal tubules. Original magnification × 400. Bars = 25 μm.

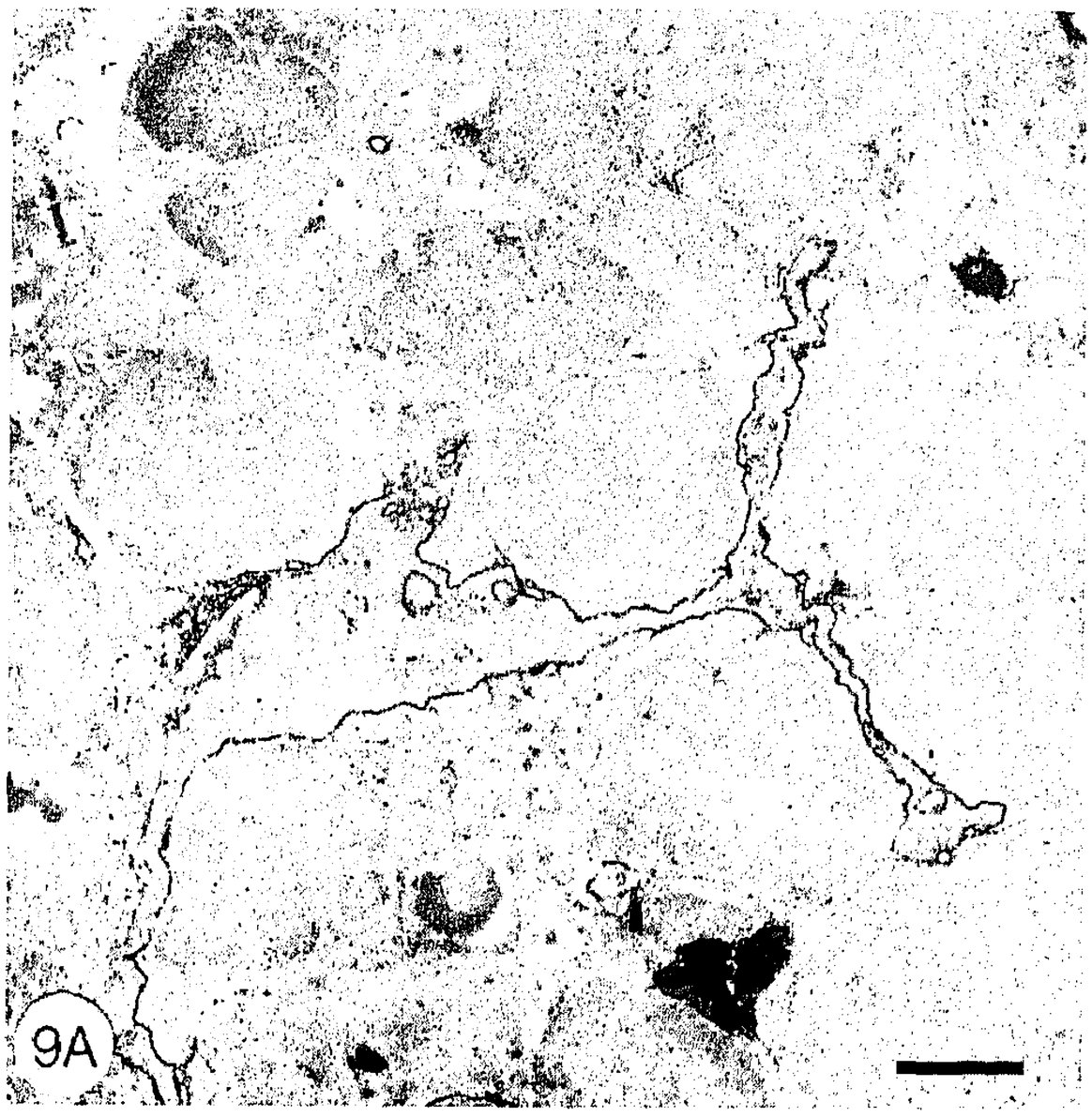

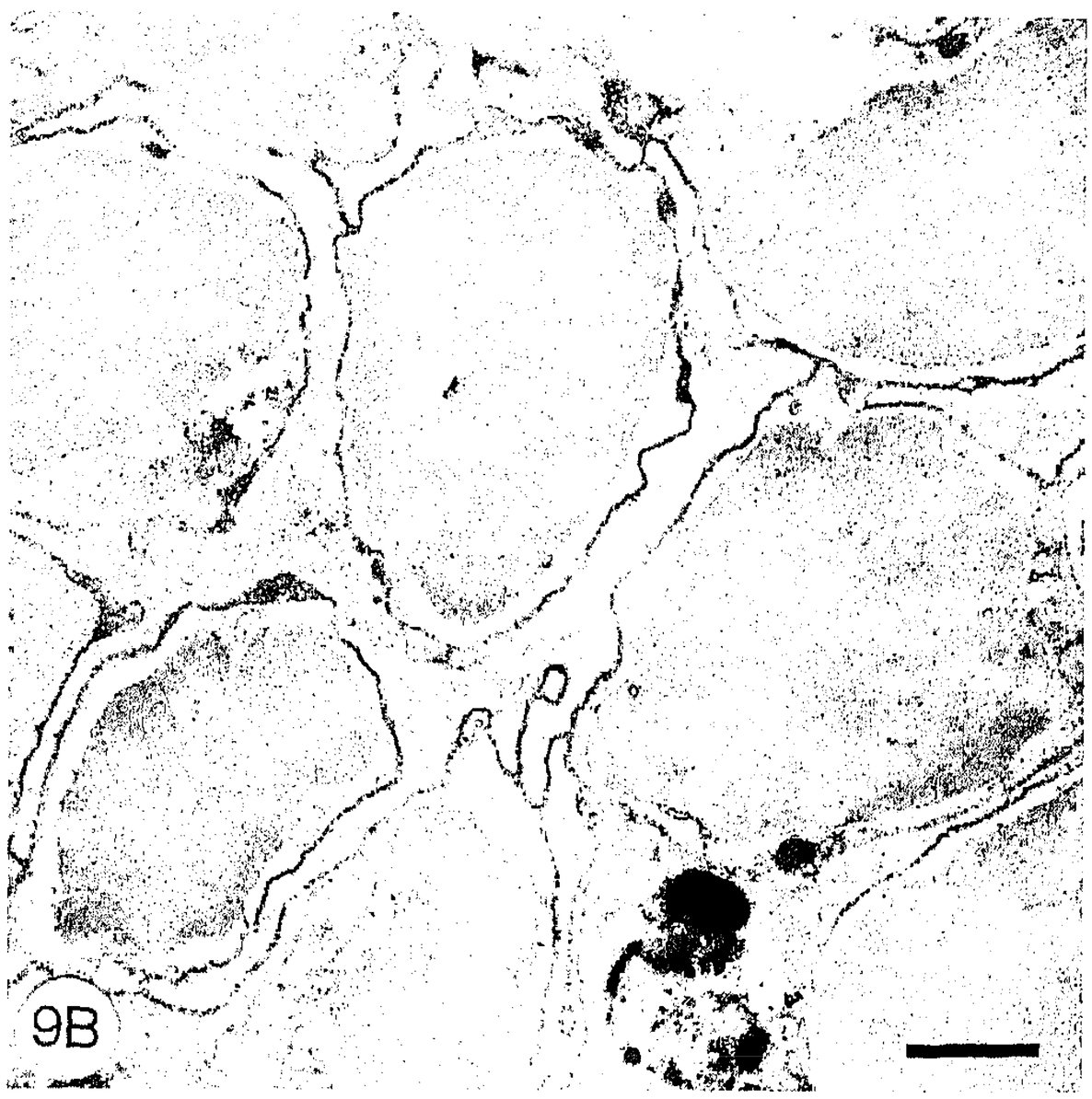

Figure 9. Indirect immunoelectron microscopy showing the binding of an MAb against APA (**A**, ASD-4) and DPP IV (**B**, ASD-36) to cortical cells of mouse thymus. **(A)** Among negative thymocytes, a dendritic process of an epithelial cell demonstrates staining of the cell membrane. **(B)** A cluster of round and oval thymocytes with relatively large nuclei shows cell membrane staining. Original magnifications: **A** × 4800; **B** × 9800. Bars: **A** = 2 μm; **B** = 1 μm.

shown that the hemodynamic effects of angiotensin II are regulated via the AT1 receptor (60). In the kidney, the presence of the AT1 receptor is closely associated with the presence of APA, i.e., the glomerulus, the juxtaglomerular cells, the proximal tubule epithelial cells, the endothelial cells of the peritubular capillaries, and the arteriolar smooth muscle cells. This supports a regulatory role for APA on the actions of angiotensin II in the kidney. Recently, we have found evidence for this in an anti-APA-mediated glomerulonephritis in the mouse (7). A single IV injection of ASD-4, an MAb that can block the enzymatic activity after binding to APA, induces an acute albuminuria that is not dependent on well-known systemic mediators, such as complement, platelets, fibrin, neutrophils, or monocytes. Treatment with the angiotensin-converting enzyme inhibitor enalapril and the AT1 receptor antagonist losartan considerably reduced this albuminuria, strongly indicating a role of angiotensin II in this model (61). We presume that blocking of the glomerular APA activity causes a prolonged effect of angiotensin II on the glomerular hemodynamics or glomerular filter, leading to enhanced permeability for proteins. A function of APA in several forms of chronic nephropathy is also suggested by others who found an association between the extent of the glomerular lesions and the reduction of the APA activity as determined by enzyme histochemistry (22).

DDP IV is a heterodimer composed of two noncovalently linked, structurally related subunits that could be immunoprecipitated by ASD-36 from the kidney and thymus. The different molecular weights ranging from 103 to 116 KD, as analyzed in SDS-PAGE under reducing conditions, largely correspond with the state of glycosylation, as reported (62). The assumption that differences in glycosylation are the basis for the differences in molecular weight of DPP IV is supported by the fact that only a single protein can be precipitated from thymus and kidney (63,64), which is encoded by a single cDNA and can be digested with glycolytic enzymes, resulting in the predicted 87.5-KD protein backbone (23,50). This is also supported by the fact that only a single DPP IV RNA isoform has been identified in kidney and thymus (62). Nevertheless, it has been described that a different cDNA coding for a variant DPP IV isoform (DPPX-L) has been cloned from bovine brain, but this iso-

Figure 8. Indirect immunofluorescence and enzyme histochemistry on murine thymus. **(A,B)**. Double staining of 2-μm-thick sections of mouse thymus incubated with MAbs against APA (**A**, ASD-4), and against cytokeratin 2/8 (**B**, RCK 102). Binding of the MAbs is detected by a second FITC-labeled anti-rat and TRITC-labeled anti-mouse antibody, respectively. APA is expressed solely on epithelial cells in the cortex of mouse thymus, as evidenced by the identical localization of cytokeratin that additionally is expressed in medullary epithelial cells. **(C,E)**. Sections of the cortex of mouse thymus stained with MAbs against APA **(C)** and DPP IV **(E)**. Binding of the MAb is visualized by an FITC-labeled anti-rat antibody. APA is present on dendrite-like epithelial cells, whereas DPP IV is localized on thymocytes. **(D,F)**. Enzyme histochemistry staining of 5-μm-thick section of mouse thymus. Cells in the cortex of the thymus, which were stained with an MAb against APA by IF **(C)**, also showed enzyme activity for APA **(D)** by enzyme histochemistry using an APA-specific substrate. Cortical cells stained with an MAb against DPP IV by IF **(E)** also showed enzyme activity for DPP IV **(F)** using a DPP IV-specific substrate. Original magnifications: **A,B** × 125; **C–F** × 350. Bars: **A,B** = 100 μm; **C–F** = 25 μm.

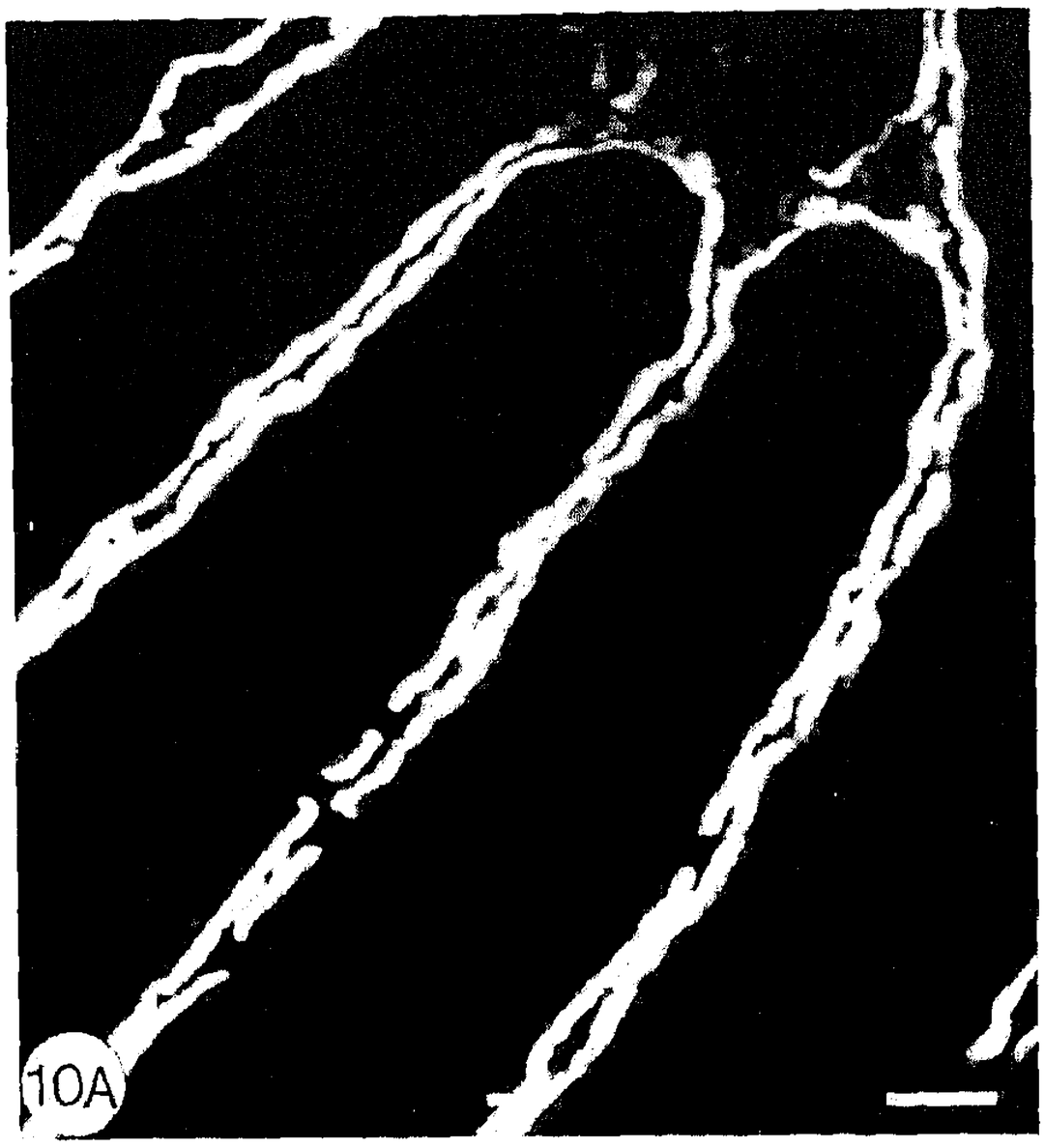

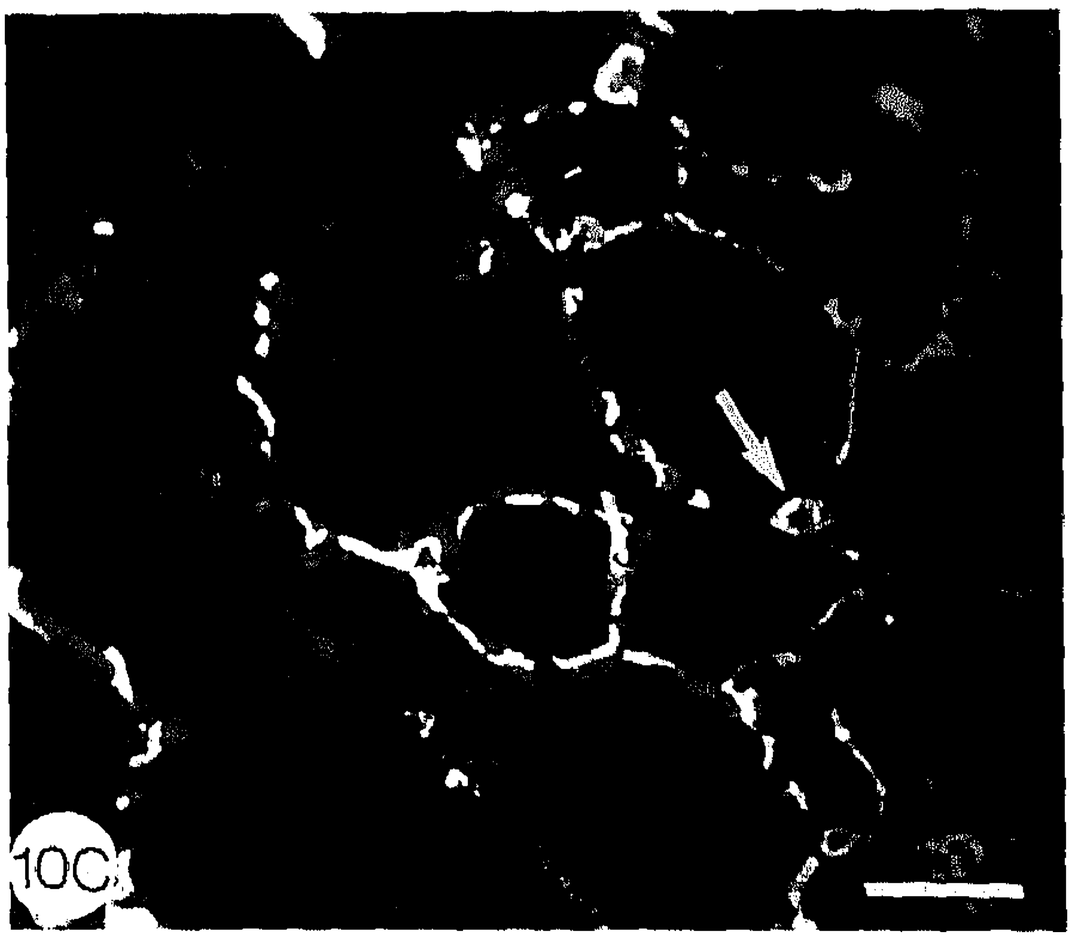

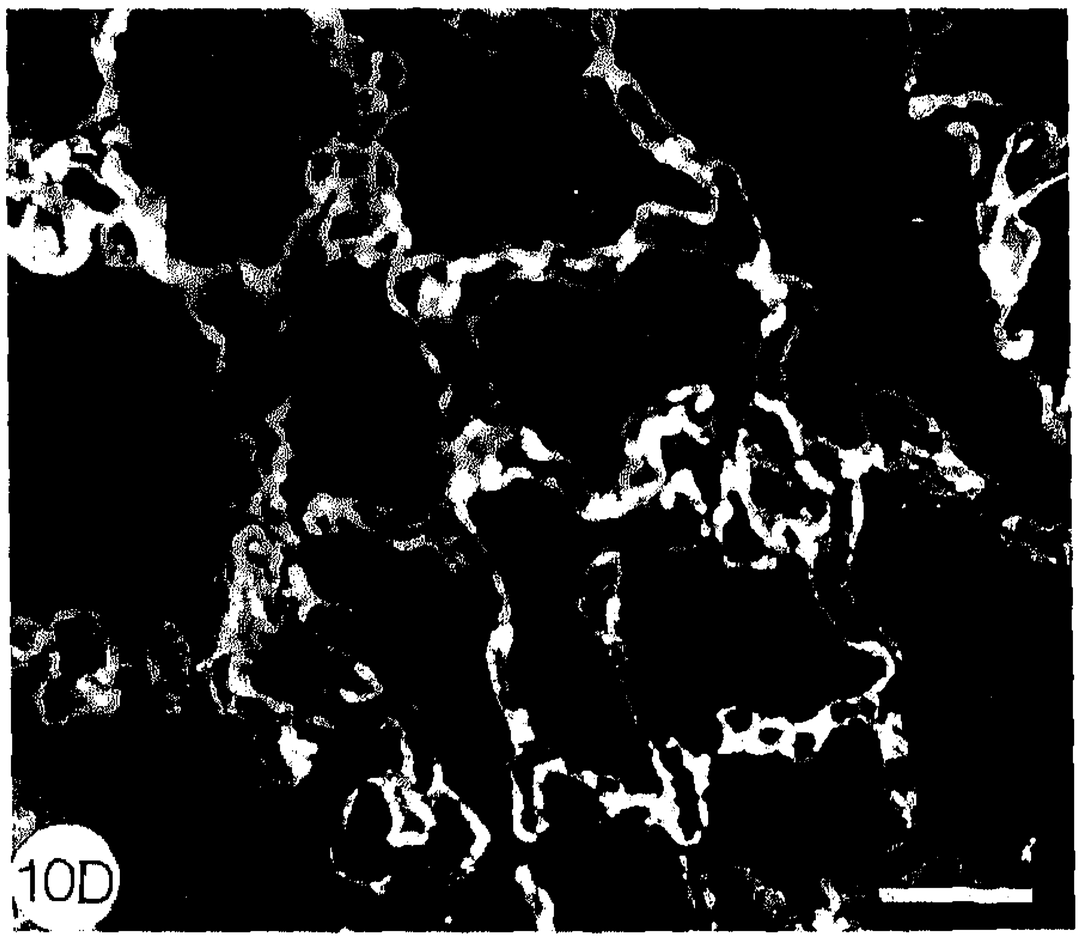

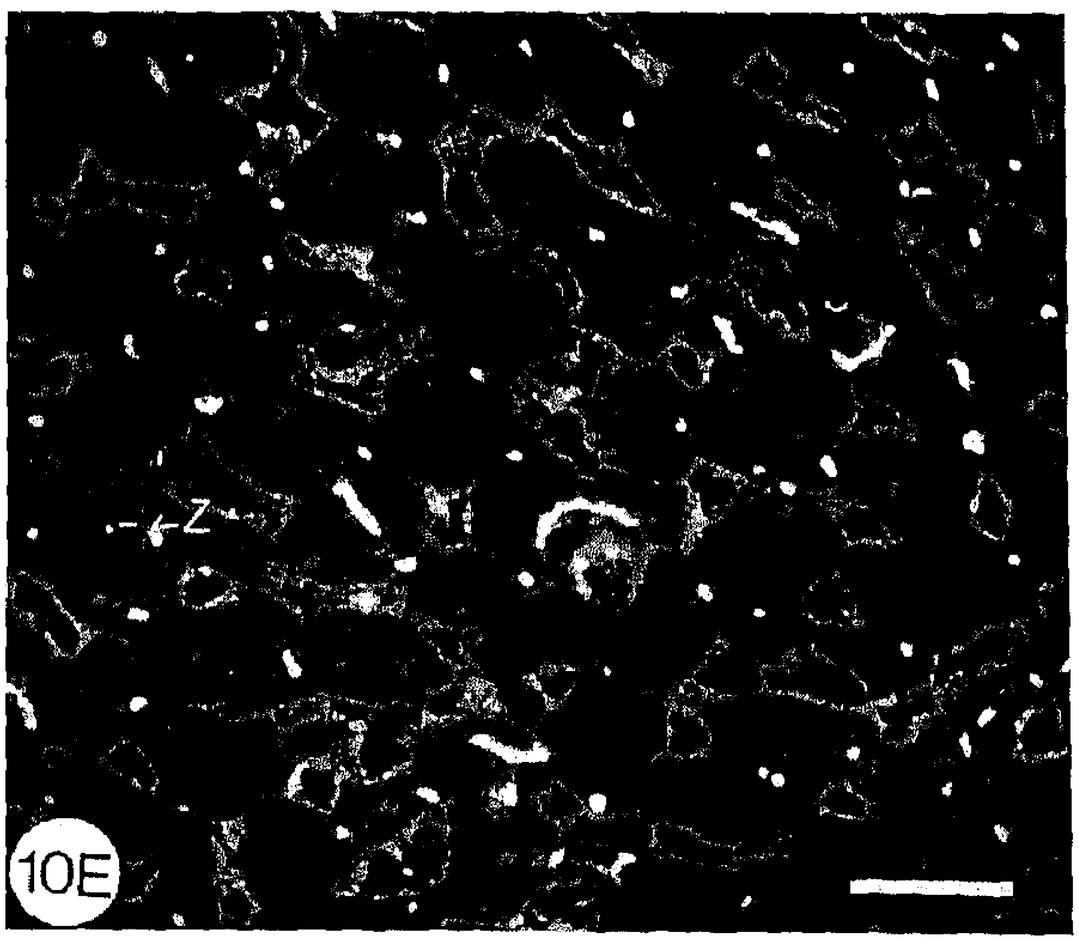

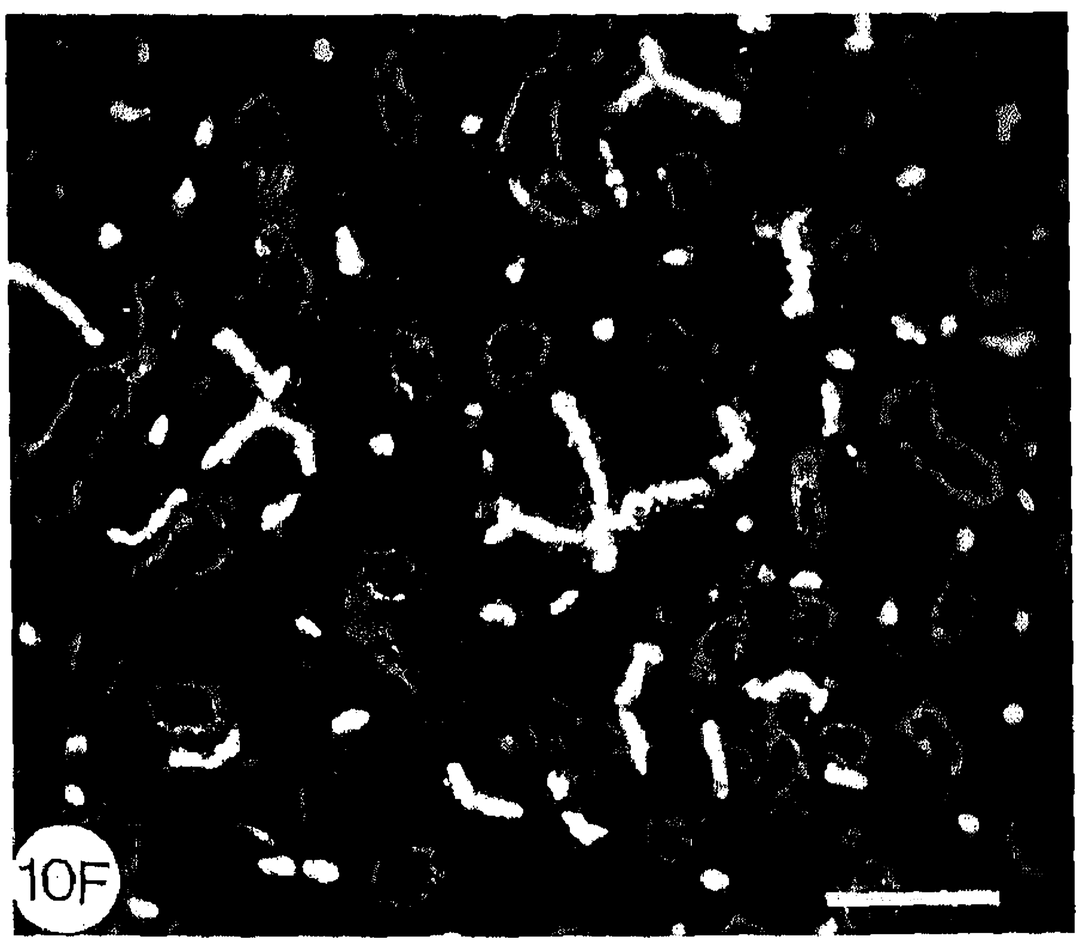

Figure 10. Indirect immunofluorescence of a normal Balb/c intestine **(A,B)**, lung **(C,D)**, and liver **(E,F)** incubated with ASD-4 **(A,C,E)** and ASD-36 **(B,D,F)**. **(A,B)** Strong homogeneous binding of the cell membranes of the brush borders of the small intestine after incubation with ASD-4. **(A)** and ASD-36 **(B)** ASD-4 stains only the endothelial cells of the lung and the large alveolar cells (arrow) **(C)**. ASD-36 stains predominantly the small alveolar cells **(D)**. In the liver, both ASD-4 **(E)** and ASD-36 **(F)** faintly stain the sinusoidal lining cells and the bile canaliculi, although staining of these latter structures was stronger after staining with ASD-36. Original magnifications: **A** × 300; **B** × 260; **C,D** × 450; **E,F** × 500. Bars = 25 μm.

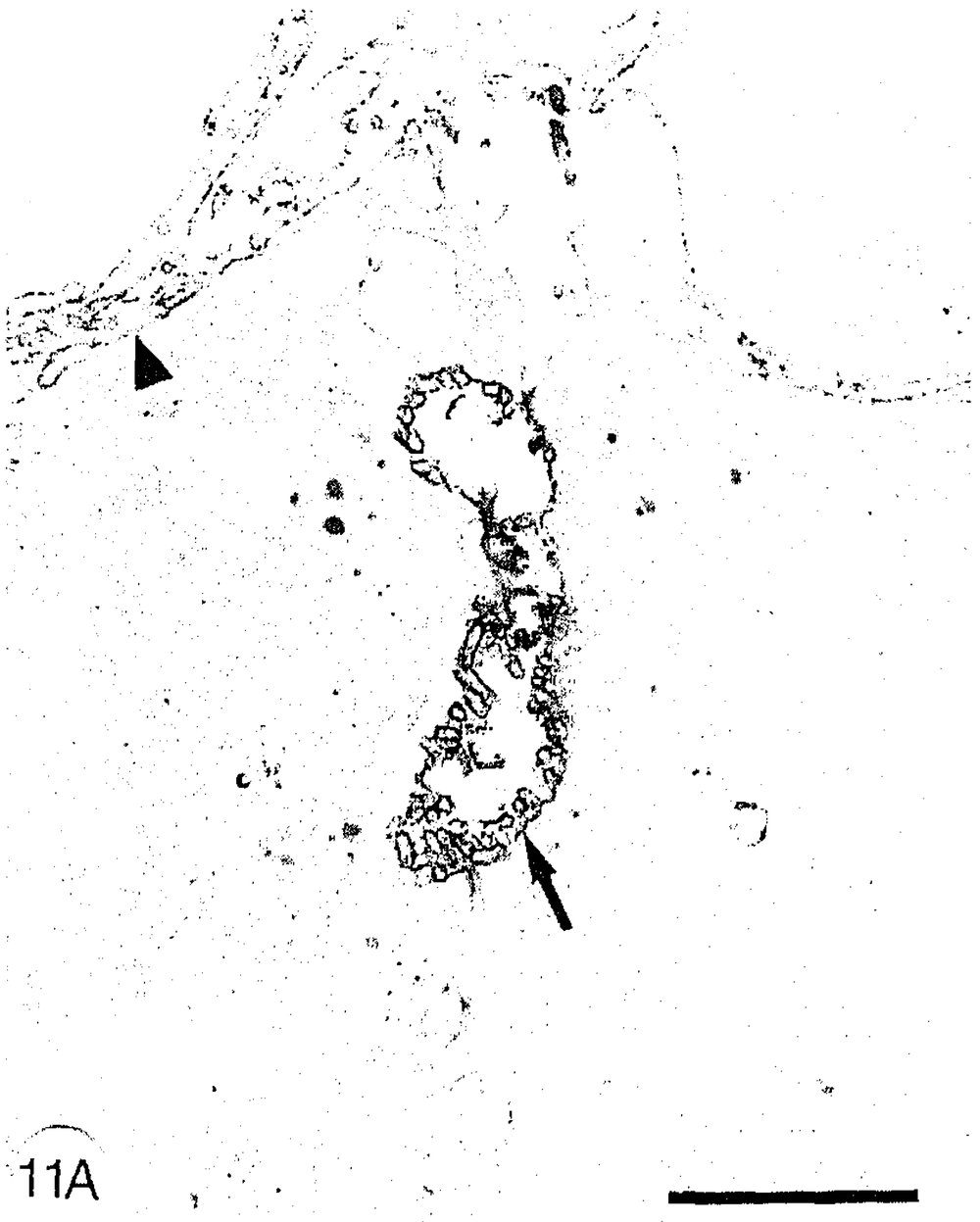

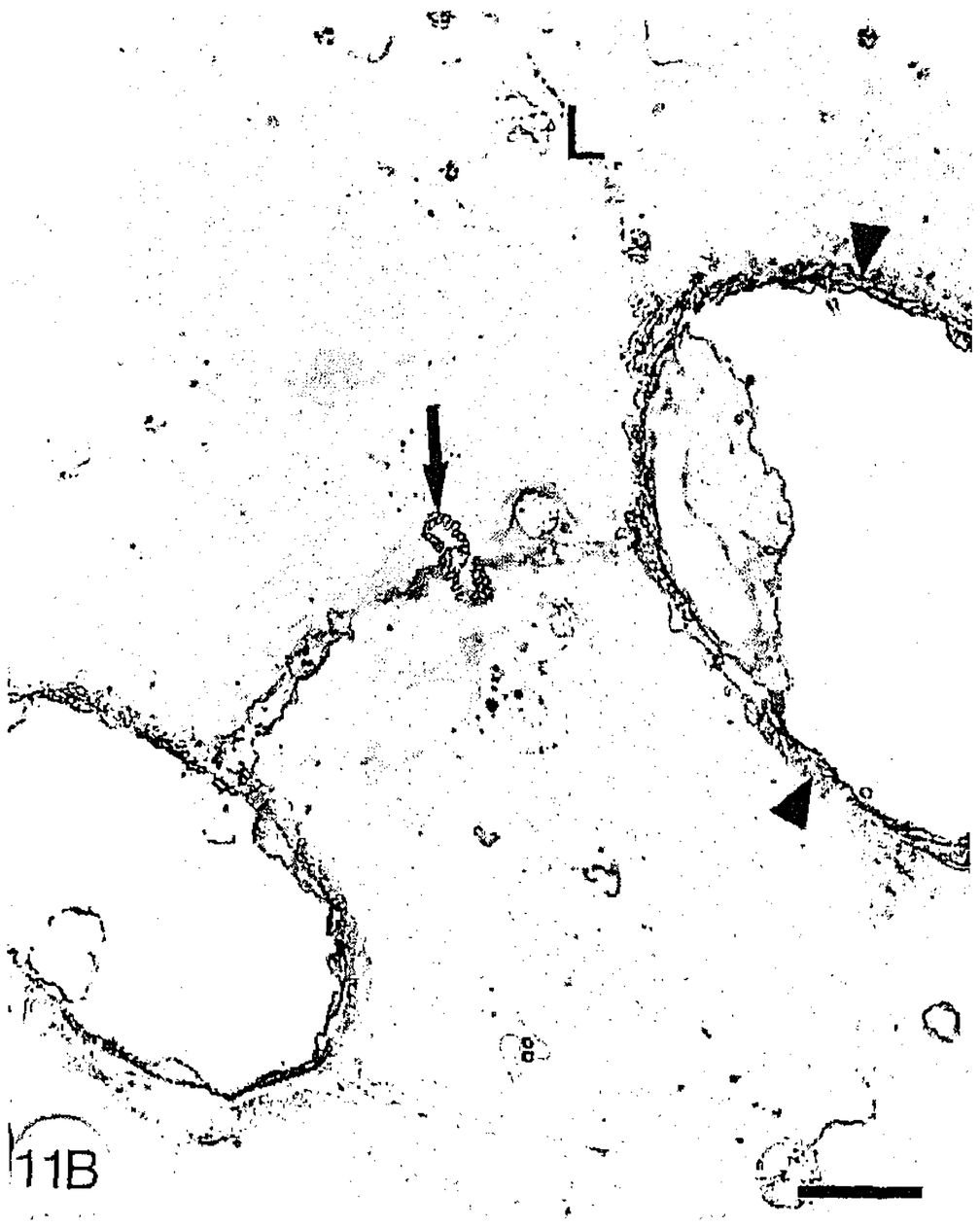

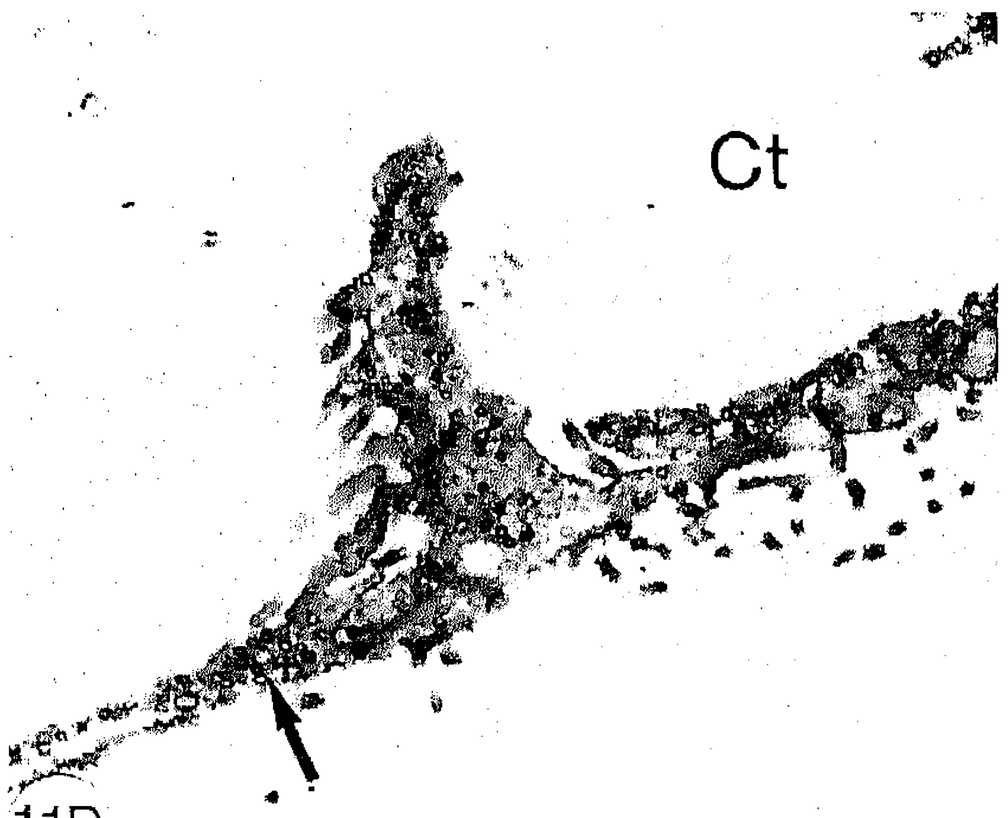

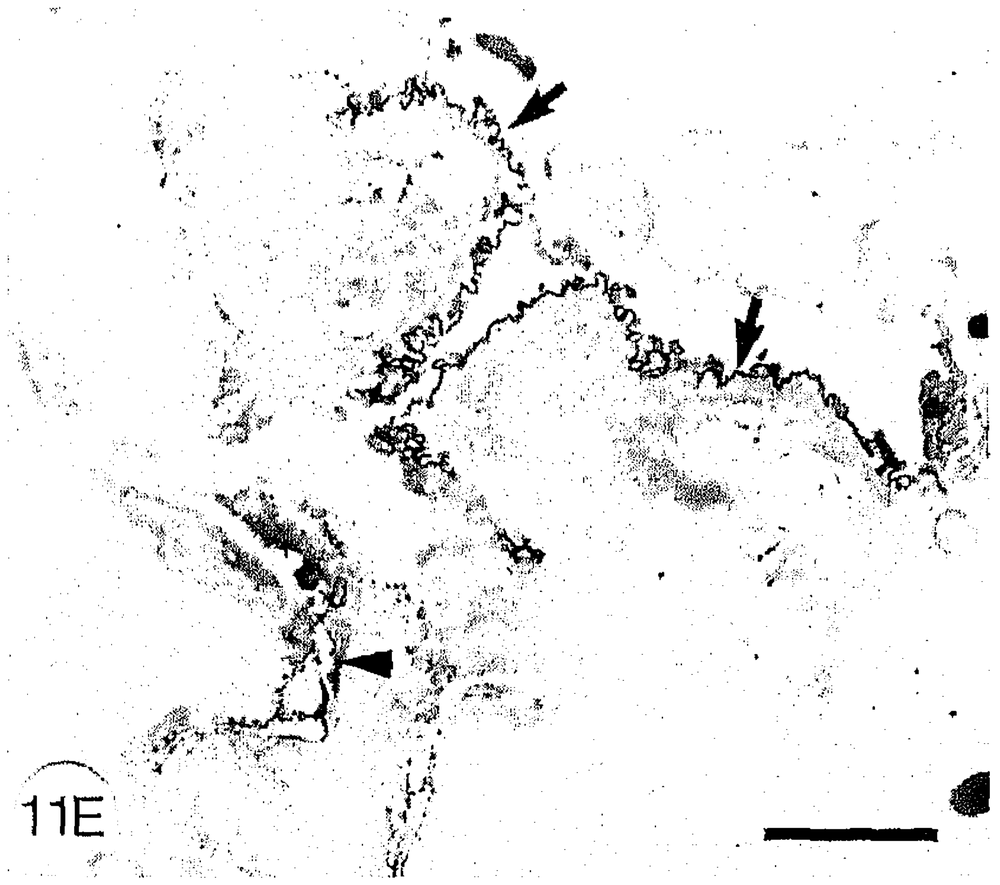

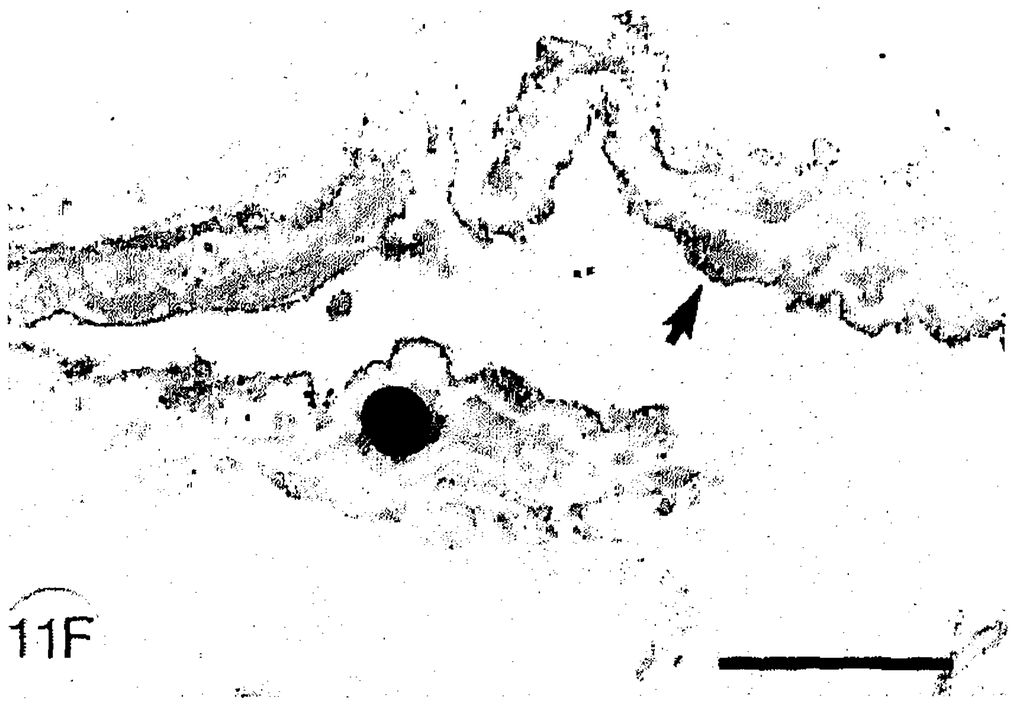

Figure 11. Indirect immunoelectron microscopy of a normal Balb/c liver **(A,B)**, small intestine **(C,D)**, and lung **(E,F)** incubated with ASD-4 **(A,C,E)** and ASD-36 **(B,D,F)**. *Immunoperoxidase labeling.* Both ASD-4 **(A)** and ASD-36 **(B)** stain the cell membranes of the bile canaliculi (arrows), the sinusoidal lining cells (arrowheads), and the liver cells (L). ASD-4 diffusely stained the brush borders of the small intestine and some extracellular material **(C)**. In addition, ASD-36 stained the mesothelial cells covering the peritoneal cavity **(D)**. Note the many stained vacuoles in the cytoplasm (arrow). *Ct, connective tissue. In the lung, the large alveolar cells (arrows) and endothelial cells (arrowhead)* are stained by ASD-4 **(E)**, whereas ASD-36 binds predominantly to the small alveolar cells (arrow) **(F)**. Original magnifications: **A** × 10,000; **B** × 4800; **C** × 4600; **D** × 12,000; **E** × 6800; **F** × 9000. Bars = 2 μm.

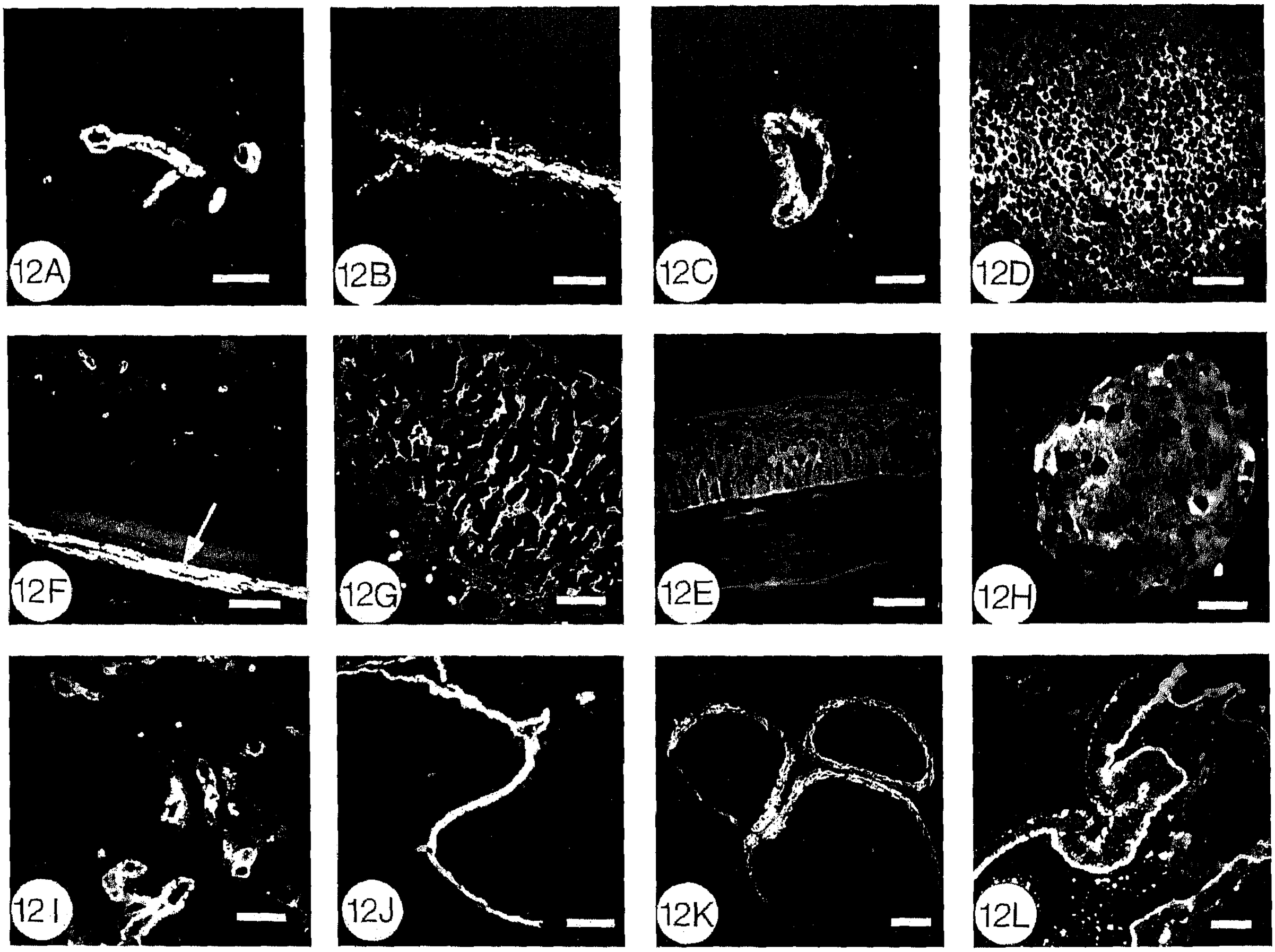

Figure 12. Indirect immunofluorescence of various organs of a normal Balb/c mouse incubated with ASD-4 or ASD-36. **(A)** Cerebrum; staining of the endothelial cells by ASD-4. **(B)** Cerebrum; ASD-36 stains astrocytes in the cortex. **(C)** Spleen; ASD-4 stains smooth muscle cells of arterioles **(D)**. Spleen; staining of T-cells around the arterioles by ASD-36. **(E)** Eye; ASD-4 binds to the epithelial and stromal cells of the cornea. **(F)** Eye; ASD-4 also binds to the choroid plexus (arrow) and endothelial cells of the retina. **(G)** Adrenal; ASD-4 stains sinusoidal lining cells of the cortex. **(H)** Pancreas; DPP IV is present in the cells of the Langerhans' islets. **(I)** Uterus; ASD-4 stains epithelial cells of the mucosal ducts. **(J)** Uterus; ASD-36 stains mainly the mucosal cells lining the uterine cavity. **(K)** Ovary; luteal cells of the follicles are positive for ASD-4. **(L)** Prostate; staining of the epithelial cells of the ducts by ASD-36. Original magnifications: **A** × 300; **B,C** × 125; **C–F,H–J** × 250; **K** × 100; **L** × 200. Bars: **A,C–F,H–J,L** = 25 μm; **B,G,K** = 50 μm.

form is expressed predominantly in brain (65). Mouse DPP IV cDNA predicts a Type II, 760–amino-acid, membrane-bound glycoprotein with a calculated size of 87 KD and with a large extracellular and a short cytoplasmic domain (62). It is a multifunctional molecule involved in signal transduction, hydrolysis and uptake of peptides, and cell adhesion. DPP IV is a serine proteinase that N-terminally digests peptides and proteins with penultimate proline or alanine residues (66). DPP IV is known to hydrolyze many natural proline-containing peptides such as cytokines, growth factors, hormones, neurotransmitters, and vasoactive components, indicating its important role in regulatory processes. Many brain, kidney, and intestinal peptides contain a penultimate proline or alanine residue that makes them susceptible to hydrolysis (23,24). Like APA, DPP IV participates in the final degradation and uptake of proline-containing peptides in the renal proximal tubules and small intestine. The necessity of intact DPP IV activity in this process was nicely demonstrated in the Fischer 344 rat strain, which lacks functional DPP IV and shows reduced digestion of proline-containing peptides in kidney and small intestine (67). DPP IV was originally known as a T-cell differentiation marker designated as CD26. It is the only ectoenzyme that functions as a co-signaling molecule in the process of T-cell activation and proliferation (68). For the signaling function, the enzymatic activity of DPP IV is not required (69). DPP IV, however, is unable to stimulate T-cells by itself but requires the expression of the T-cell receptor (TCR)/CD3 complex (70). DPP IV may also function as an auxiliary adhesion molecule, because it can bind with low affinity to the extracellular matrix components fibronectin and collagen (14,71). Recently, a role for DPP IV in the uptake of the human immunodeficiency virus in $CD4^+$ T-cells has been proposed (72). Finally, DPP IV appears to

participate in some forms of membranous glomerulonephritis in the mouse and rat (6,8,11–14,16,73,74). However, in contrast to the well-defined role of APA in the passive glomerulonephritis in mice, the involvement of DPP IV in several experimental forms of glomerulonephritis is controversial at the moment and is not well understood. Using polyclonal and monoclonal anti-mouse DPP IV antibodies, we could induce a membraneous glomerulonephritis morphologically characterized by granular immune deposits in the subepithelial space of the glomerulus and without the involvement of systemic mediators. However, we never could induce a sustained enhanced glomerular permeability as seen in our anti-APA model or in the Heymann nephritis model in the rat. In the membranous glomerulonephritis in the so-called graft-vs-host mice, it was suggested that DPP IV was also involved in the formation of the immune complexes in the glomerulus, but we could not confirm this observation (17,18,75). Moreover, the participation of this enzyme as an additional antigen next to the Heymann antigen in the induction of the Heymann nephritis is controversial (15,76). The function of DPP IV in the glomerulus is not fully understood at present. It is also not known whether DPP IV acts as an ectoenzyme or as an adhesion molecule in the various forms of glomerulonephritis.

In the thymus, APA is localized on cortical epithelial cells, whereas DPP IV is present on thymocytes. It is known that progenitors of T-lymphocytes develop into mature T-cells characterized by a rearranged T-cell receptor/CD3 complex and the CD4 or CD8 molecules, by interacting with a variety of stromal or epithelial cells that compose the microenvironment of the thymus (77). It is believed that these stromal cells in the thymic cortex provide specific signals in the T-cell differentiation that starts beneath the subcapsular region and evolves along the cortex to the medulla. Epithelial cells with their cytoplasmic extensions are organized in an elaborate network along which the thymocytes migrate during the differentiation process. How these stromal cells act on the development of T-cells is not well understood, but it is assumed that cell-associated MHC antigens play an important role in this process of maturation, requiring a direct contact between thymocytes and stromal cells. The cortical thymocytes that show high $CD4^+/8^+$ expression and no or low TCR expression are submitted to an MHC-restricted "positive" selection and a tolerance-inducing "negative" selection before they become a mature T-cell population that recognizes peptides only in the context of self (77–79). Which role APA plays in the maturation of thymocytes is completely unknown at the moment. DPP IV in the thymus is known as a co-stimulatory molecule of thymocytes, possibly in association with other activating factors such as IL-2 and CD4 or CD8 (64,80). Although the strict separation in expression of APA and DPP IV suggests some form of counteractive enzymatic activity between the cortical epithelial cells and thymocytes, such an effect remains to be confirmed.

Acknowledgment

We thank Mr J. Koedam for excellent technical assistance.

Literature Cited

1. Brentjens JR, Andres GA. Interaction of antibodies with renal cell surface antigens. Kidney Int 1989;35:954–968
2. Couser WG. Mediation of immune glomerular injury. J Am Soc Nephrol 1990;1:13–29
3. Kerjaschki D, Farquhar MG. The pathogenic antigen of Heymann nephritis is a membrane glycoprotein of the renal proximal tubule brush border. Proc Natl Acad Sci USA 1982;79:5557–5561
4. Kerjaschki D, Farquhar MG. Immunocytochemical localization of the Heymann nephritis antigen (gp330) in glomerular epithelial cells of normal Lewis rats. J Exp Med 1983;157:667–686
5. Kerjaschki D. Molecular pathogenesis of membranous nephropathy. Kidney Int 1992;41:1090–1105
6. Assmann KJM, Ronco P, Tangelder MM, Lange WPH, Verroust P, Koene RAP. Comparison of antigenic targets involved in antibody-mediated membraneous glomerulonephritis in the mouse and rat. Am J Pathol 1985;121:112–122
7. Assmann KJM, van Son JPHF, Dijkman HBPM, Koene RAP. A nephritogenic rat monoclonal antibody to mouse aminopeptidase A. Induction of massive albuminuria after a single intravenous injection. J Exp Med 1992;175:623–635
8. Assmann KJM, Ronco P, Tangelder MM, Lange WPH, Verroust P, Koene RAP. Involvement of an antigen distinct from the Heymann antigen in membranous glomerulonephritis in the mouse. Lab Invest 1989; 60:138–146
9. Assmann KJM, Tangelder MM, Lange WPH, Tadema TM, Koene RAP. Membranous glomerulonephritis in the mouse. Kidney Int 1983;24: 303–312
10. Wolf GB, Thaiss F, Scherberich JE, Schoeppe W, Stahl RAK. Glomerular angiotensinase A in the rat: increase of enzyme activity following renal ablation. Kidney Int 1990;38:862–868
11. Mendrick DL, Rennke HG. Induction of proteinuria in the rat by a monoclonal antibody against SGP-115/107. Kidney Int 1988;33:818–830
12. Natori Y, Hayakawa I, Shibata S. Passive Heymann nephritis with acute and severe proteinuria induced by heterologous antibody against renal tubular brush border glycoprotein gp 108. Lab Invest 1986;55:63–70
13. Ronco P, Allegri L, Melcion C, Pirotsky E, Appay M, Bariety J, Pontillon F, Verroust P. A monoclonal antibody to brush border and passive Heymann nephritis. Clin Exp Immunol 1984;55:319–332
14. Hogendoorn PCW, Bruijn JA, van den Broeck LJCM, de Heer E, Foidart JM, Hoedemaeker PHJ, Fleuren GJ. Antibodies to purified renal tubular antigens contain activity against laminin, fibronectin and type IV collagen. Lab Invest 1988;58:831–842
15. Bagchus WM, Hoedemaeker PJ, Siegers JFG, Baker WW. The specificity of nephritogenic antibodies. V. Glomerular localization of anti-gp330 and anti-gp90 antibodies present in passive Heymann serum. Br J Exp Pathol 1988;69:855–864
16. van Leer EHG, de Roo GM, Bruijn JA, Hoedemaeker PHJ, de Heer E. Synergistic effects of anti-gp330 and dipeptidyl peptidase type IV antibodies in the induction of glomerular damage. Exp Nephrol 1993; 1:292–300
17. Bruijn JA, van Leer EHG, Baelde HJJ, Corver WE, Hogendoorn PCW, Fleuren GJ. Characterization and in vivo transfer of nephritogenic autoantibodies directed against dipeptidyl peptidase IV and laminin in experimental lupus nephritis. Lab Invest 1990;63:350–359
18. van Leer EHG, Bruijn JA, Prins FA, Hoedemaeker PJ, de Heer E. Redistribution of glomerular dipeptidyl peptidase IV in experimental lupus nephritis. Lab Invest 1993;68:550–556.
19. Scherberich JE, Matthess A, Remelius W, Schoeppe W. Aminopeptidase A (= angiotensinase A) in human progressive renal disease. Miner Electrolyte Metab 1992;18:97–100
20. Nukada O, Kobayashi M, Moriwake T, Kanzaki S, Himei H, Yoda T, Seino Y. Urinary glycylprolyl dipeptidyl aminopeptidase (GP-DAP) in insulin-dependent diabetic patients. Acta Paediatr 1992; 81:907–911

21. Scherberich JE, Wolf GB, Albers C, Nowack A, Stuckhardt C, Schoeppe W. Glomerular and tubular membrane antigens reflecting cellular adaptation in human renal failure. Kidney Int 1989;36:S38–S51
22. Scherberich JE, Wiemer J, Schoeppe W. Biochemical and immunological properties of urinary angiotensinase A and dipeptidylaminopeptidase IV. Their use as markers in patients with renal cell injury. Eur J Clin Chem Clin Biochem 1992;30:663–668
23. Shipp MA, Look AT. Hematopoietic differentiation antigens that are membrane-associated enzymes: cutting is the key! Blood 1993;82:1052–1070
24. Kenny AJ, Stephenson SL, Turner AJ. Cell surface peptidases. In Kenny AJ, Turner AJ, eds. Mammalian ectoenzymes. Amsterdam: Elsevier Science Publishers, 1987:169–210
25. Tidmarsh GF, Dailey MO, Whitlock C, Pillemer , Weissman IL. Transformed lymphocytes from Abelson-diseased mice express levels of a B-lineage transformation-associated antigen elevated from that found on normal lymphocytes. J Exp Med 1985;162:1421–1434
26. Kugler P. Localization of aminopeptidase A (angiotensinase A) in the rat and mouse kidney. Histochemistry 1981;72:269–278
27. Lojda Z, Gossrau R. Study of aminopeptidase A. Histochemistry 1980; 67:267–290
28. Li L, Wu Q, Wang JY, Bucy RP, Cooper MD. Widespread tissue distribution of aminopeptidase A, an evolutionarily conserved ectoenzyme recognized by the Bp-1 antibody. Tissue Antigens 1993;42:488–496
29. Gossrau R. Peptidasen II. Zur Lokalisation der Dipeptidylpeptidase IV (DPP IV). Histochemische und biochemische Untersuchung. Histochemistry 1979;60:231–248
30. Chatelet F, Brianti E, Ronco P, Roland J, Verroust P. Ultrastructural localization by monoclonal antibodies of brush border antigens expressed by glomeruli. II. Extrarenal distribution. Am J Pathol 1986;122:512–519
31. Assmann KJM, Lange WPH, Tangelder MM, Koene RAP. The organ distribution of gp-330 (Heymann antigen) and gp-90 in the mouse and rat. Virchows Arch 1986;408:541–553
32. Malathi P, Preiser H, Fairclough P, Mallett P, Crane RK. A rapid method for the isolation of kidney brush border membrane. Biochim Biophys Acta 1979;554:259–263
33. Bordier C. Phase separation of integral membrane proteins in Triton X-114 solution. J Biol Chem 1981;256:1604–1607
34. Assmann KJM, van Son JPHF, Koene RAP. Improved method for the isolation of mouse glomeruli. J Am Soc Nephrol 1991;2:944–946
35. Lowry OH, Rosebrough RL, Farr RL, Randall RJ. Protein measurement with the Folin phenol reagent. J Biol Chem 1951;193:265–275
36. Köhler G, Milstein C. Continuous cultures of fused cells secreting antibody of predefined specificity. Nature 1975;256:495–497
37. Mancini G, Carbonara AO, Heremans JF. Immunochemical quantitation of antigens by single radial immunodiffusion. Immunochemistry 1965;2:235–254
38. Coombs RRA, Scott ML, Cranage MP. Assays using red cell-labeled antibodies. J Immunol Methods 1987;101:1–14
39. Tauc M, Chatelet F, Verroust P, Vandewalle A, Poujeol P, Ronco P. Characterization of monoclonal antibodies specific for rabbit renal brush-border hydrolases: application to immunohistological localization. J Histochem Cytochem 1988;36:523–532
40. Markwell MAK. A new solid state reagent to iodinate proteins. 1. Conditions for the efficient labeling of antiserum. Anal Biochem 1982; 125:427–432
41. Laemmli UK. Cleavage of structural proteins during the assembly of the head of bacteriophage T_4. Nature 1970;227:680–685
42. Verroust P, Ronco P, Chatelet F. Antigenic targets in membranous glomerulonephritis. Springer Semin Immunopathol 1987;9:341–358
43. Castillo MJ, Nakajima K, Zimmerman M, Powers JC. Sensitive substrates for human leucocyte and porcine pancreatic elastase: a study of the merits of various chromophoric and fluorogenic groups in assays for serine proteases. Anal Biochem 1979;99:53–64
44. Laitinen L, Virtanen I, Saxen L. Changes in glycosylation pattern during embryonic development of mouse kidney as revealed with lectin conjugates. J Histochem Cytochem 1989;35:55–65
45. Broers JLV, Carney DN, Klein Rot M, Schaart G, Lane EB, Vooys GP. Intermediate filament proteins in classic and variant types of small cell lung carcinoma cell lines: a biochemical and immunochemical analysis using a panel of monoclonal and polyclonal antibodies. J Cell Sci 1986;83:37–60
46. Cooper MD, Mulvaney D, Coutinho A, Cazenave P. A novel cell surface molecule on early B-lineage cells. Nature 1986;321:616–618
47. Kameoka J, Tanaka T, Nojima Y, Schlossman SF, Morimoto C. Direct association of adenosine deaminase with a T cell activation antigen, CD26. Science 1993;261:466–469
48. Mentzel S, de Leeuw EPH, van Son JPHF, Dijkman HBPM, Koene RAP, Assmann KJM. Actin is directly associated to aminopeptidase A (APA) in brush border membranes from mouse kidney. Hoppe Seylers Biol Chem 1994;375:623–627
49. Geppert TD, Davis LS, Gur H, Wacholtz MC, Lipsky PE. Accessory cell signals involved in T-cell activation. Immunol Rev 1990;117:5–66
50. Fleischer B. CD26—a surface protease involved in T-cell activation. Immunol Today 1994;15:180–184
51. Wu Q, Lahti JM, Air GM, Burrows PD, Cooper MD. Molecular cloning of the murine BP-1/6C3 antigen: a member of the zinc-dependent metallopeptidase family. Proc Natl Acad Sci USA 1990;87:993–997
52. Wu Q, Tidmarsh GF, Welch PA, Pierce JH, Weissman IL, Cooper MD. The early B lineage antigen Bp-1 and the transformation-associated antigen 6C3 are on the same molecule. J Immunol 1990;143:3303–3308
53. Glenner GG, McMillan PJ, Folk JE. A mammalian peptidase specific for the hydrolysis of N-terminal α-L-glutamyl and aspartyl residues. Nature 1962;194:867
54. Sherwood PJ, Weissman IL. The growth factor IL-7 induces expression of a transformation-associated antigen in normal pre-B cells. Int Immunol 1990;2:399–406
55. Ulmer AJ, Mattern T, Flad HD. Expression of CD26 (dipeptidyl peptidase IV) on memory and naive T lymphocytes. Scand J Immunol 1992;35:551–559
56. Erdos EG, Skidgel RA. Renal metabolism of angiotensin I and II. Kidney Int 1994;38:S24–S27
57. Ichikawa I, Harris RC. Angiotensin actions in the kidney: renewed insight into the old hormone. Kidney Int 1991;40:583–596
58. Douglas JG, Hopfer U. Novel aspect of angiotensin receptors and signal transduction in the kidney. Annu Rev Physiol 1994;56:649–669
59. Smith RD, Timmermans PBMWM. Human angiotensin receptor subtypes. Curr Opin Nephrol Hypertens 1994;3:112–122
60. Reid IA, Morris BJ, Ganong WF. The renin-angiotensin system. Annu Rev Physiol 1978;40:377–410
61. Mentzel S, Assmann KJM, van Son JPHF, Dijkman HBPM, Koene RAP. Enalapril and losartan reduce considerably the acute albuminuria induced by injection of a monoclonal antibody against aminopeptidase A. J Am Soc Nephrol 1993;4:620
62. Marguet D, Bernard A, Vivier I, Darmoul D, Naquet P, Pierres M. cDNA cloning for mouse thymocyte-activating molecule. J Biol Chem 1992; 267:2200–2208
63. Elleder M, Stejskal J. Induction of dipeptidyl peptidase IV activity in human renal glomeruli—a histochemical study. Acta Histochem 1983; 77:75–78

64. Dang NH, Torimoto Y, Shimamura K, Tanaka T, Daley JF, Schlossman SF, Morimoto C. 1F7 (CD26): a marker of thymic maturation in the differential regulation of the CD3 and CD2 pathways of human thymocyte activation. J Immunol 1991;147:2825–2832

65. Wada K, Yokotani N, Hunter C, Doi K, Wenthold RJ, Shimasaki S. Differential expression of two distinct forms of mRNA encoding members of a dipeptidyl aminopeptidase family. Proc Natl Acad Sci USA 1992;89:197–201

66. Smith RE, Reynolds CJ, Elder EA. The evolution of proteinase substrates with special references to dipeptidylpeptidase IV. Histochem J 1992;24:637–647

67. Erickson RH, Suzuki Y, Sedlmayer A, Kim YS. Biosynthesis and degradation of altered immature forms of intestinal dipeptidyl peptidase IV in a rat strain lacking the enzyme. J Biol Chem 1992;267:21623–21629

68. Naquet P, MacDonald HR, Brekelmans P, Barber J, Marchetto S, van Ewijk W, Pierres M. A novel T cell-activating molecule (THAM) highly expressed on CD4-CD8- murine thymocytes. J Immunol 1988;141: 4101–4109

69. Hegen M, Mittrucker HW, Hug R, Demuth HU, Neubert K, Barth A, Fleischer B. Enzymatic activity of CD26 (dipeptidylpeptidase IV) is not required for its signaling function in T cells. Immunology 1993;189:483–493

70. Naquet P, Vivier I, Gorvel J, Brekelmans P, Barad M, Bernard A, Pierres M. Activation of mouse T lymphocytes by a monoclonal antibody to a developmentally regulated surface aminopeptidase (THAM). Immunol Rev 1989;111:177–193

71. Hanski C, Huhle T, Gossrau R, Reutter W. Direct evidence for the binding of rat liver DPP IV to collagen in vitro. Exp Cell Res 1988;178:64–72

72. Miyamoto Y, Ganapathy V, Barlas A, Neubert K, Barth A, Leibach FH. Role of dipeptidyl peptidase IV in uptake of peptide nitrogen from β-casomorphin in rabbit renal BBMV. Am J Physiol 1987;252:F670–F677

73. Natori Y, Hayakawa I, Shibata S. Role of dipeptidyl peptidase IV (gp108) in passive Heymann nephritis. Use of dipeptidyl peptidase IV-deficient rats. Am J Pathol 1989;134:405–410

74. Bruijn JA, van Elven EH, Hogendoorn PCW, Corver WE, Hoedemaeker PJ, Fleuren GJ. Murine chronic graft-versus-host disease as a model for lupus nephritis. Am J Pathol 1988;81:334–338

75. Termaat RM, Assmann KJM, van Son JPHF, Dijkman HBPM, Koene RAP, Berden JHM. Antigen-specificity of antibodies bound to glomeruli of mice with systemic lupus erythematosus-like syndromes. Lab Invest 1993;68:164–173

76. Susani M, Schulze M, Exner M, Kerjaschki D. Antibodies to glycolipids activate complement and promote proteinuria in passive Heymann nephritis. Am J Pathol 1994;144:807–819

77. van Ewijk W. T-cell differentiation is influenced by thymic microenvironments. Annu Rev Immunol 1991;9:591–615

78. von Boehmer H. Positive selection of lymphocytes. Cell 1994;76:219–228

79. van Ewijk W. Cell surface topography of thymic microenvironments. Lab Invest 1988;59:579–590

80. Bristol LA, Sakaguchi K, Appella E, Doyle D, Takacs L. Thymocyte costimulating antigen is CD26 (dipeptidyl peptidase IV). J Immunol 1992;149:367–372